Int J Earth Sci (Geol Rundsch) (2018) 107:1033–1058
https://doi.org/10.1007/s00531-017-1519-0

ORIGINAL PAPER

Mantle source heterogeneity of the Early Jurassic basalt of eastern North America

J. Gregory Shellnutt[1] · Jaroslav Dostal[2] · Meng-Wan Yeh[1]

Received: 21 February 2017 / Accepted: 19 July 2017 / Published online: 4 August 2017

Abstract One of the defining characteristics of the basaltic rocks from the Early Jurassic Eastern North America (ENA) sub-province of the Central Atlantic Magmatic Province (CAMP) is the systematic compositional variation from South to North. Moreover, the tectono-thermal regime of the CAMP is debated as it demonstrates geological and structural characteristics (size, radial dyke pattern) that are commonly associated with mantle plume-derived mafic continental large igneous provinces but is considered to be unrelated to a plume. Mantle potential temperature (T_P) estimates of the northern-most CAMP flood basalts (North Mountain basalt, Fundy Basin) indicate that they were likely produced under a thermal regime ($T_P \approx 1450$ °C) that is closer to ambient mantle ($T_P \approx 1400$ °C) conditions and are indistinguishable from other regions of the ENA sub-province ($T_{Psouth} = 1320$–1490 °C, $T_{Pnorth} = 1390$–1480 °C). The regional mantle potential temperatures are consistent along the 3000-km-long ENA sub-province suggesting that the CAMP was unlikely to be generated by a mantle plume. Furthermore, the mantle potential temperature calculation using the rocks from the Northern Appalachians favors an Fe-rich mantle (FeOt = 8.6 wt %) source, whereas the rocks from the South Appalachians favor a less Fe-rich (FeOt = 8.3 wt %) source. The results indicate that the spatial-compositional variation of the ENA basaltic rocks is likely related to differing amounts of melting of mantle sources that reflect the uniqueness of their regional accreted terranes (Carolinia and West Avalonia) and their post-accretion, pre-rift structural histories.

Keywords Central Atlantic Magmatic Province · North Mountain basalt · Early Jurassic · Mantle potential temperature · Northern Appalachians

Introduction

Numerous early Mesozoic continental tholeiitic basalt flows and dykes are found along the eastern margin of North America from Florida and South Carolina to Nova Scotia and Newfoundland and form part of the Newark Supergroup. The Newark Supergroup is composed of Late Triassic–Early Jurassic (Hettangian) fluvial and/or lacustrine sedimentary rocks (Froelich and Olsen 1985) that are intercalated with basaltic flows. The emplacement of the basaltic rocks occurred at ~200 Ma and lasted <1 million years (Olsen 1997; Olsen et al. 1998; Marzoli et al. 2011). The presence of a long, continuous geophysical reflector off the continental margin of North America indicates a much more extensive offshore continuation of these basalts. The basaltic rocks are part of the larger, Central Atlantic Magmatic Province (CAMP) that is exposed along the continental margins of South America, Western Europe, and West Africa (Fig. 1). The volcanic and plutonic rocks were emplaced along with sedimentary rocks within extensional basins during lithospheric extension and continental rifting that preceded the opening of the Atlantic Ocean (Dostal and

Electronic supplementary material The online version of this article (doi:10.1007/s00531-017-1519-0) contains supplementary material, which is available to authorized users.

✉ J. Gregory Shellnutt
jgshelln@ntnu.edu.tw

[1] Department of Earth Sciences, National Taiwan Normal University, 88 Tingzhou Road Section 4, Taipei 11677, Taiwan

[2] Department of Geology, Saint Mary's University, 923 Robie Street, Halifax, NS B3H 3C3, Canada

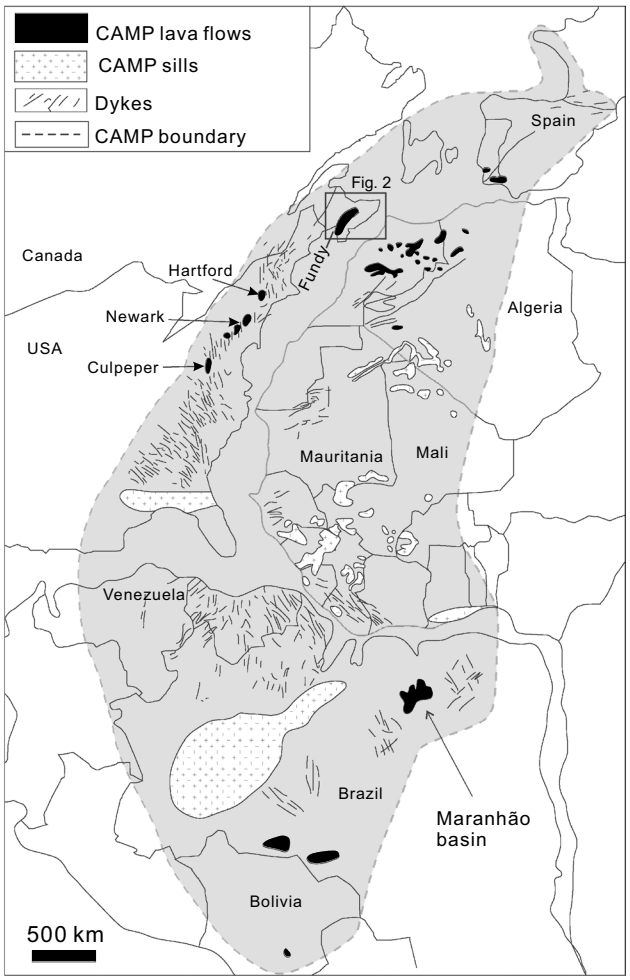

Fig. 1 Distribution of volcanic and plutonic rocks of the Central Atlantic Magmatic Province and location of the Fundy Basin. Based on Merle et al. (2013)

Durning 1998; Marzoli et al. 1999; Pe-Piper and Reynolds 2000; Whithjack et al. 2012).

The CAMP is one of the largest flood basalt provinces, covering an area $\geq 10^7$ km^2, and was contemporaneous with the end-Triassic mass extinction (Marzoli et al. 1999, 2004; Whiteside et al. 2010; Blackburn et al. 2013). The compositional variation of the mafic volcanic rocks, along with the radial nature of dykes around an inferred volcanic epicenter, is considered to be strong evidence in favor of a mantle plume origin but there remain compelling arguments against such a model (Greenough and Hodych 1990; Wilson 1997; Janney and Castillo 2001; Storey et al. 2001; Cebriá et al. 2003; Melankholina and Sushchevskaya 2015). Specifically, the thermal regime of the mantle that generated the flood basalts was not anomalously hot; there is no hotspot track, and that rifting began ~25 million years before the eruption of the basalts (McHone 2000; Callegaro et al. 2013; Hole 2015; Whalen et al. 2015).

One of the defining characteristics of CAMP basaltic rocks from the eastern North America (ENA) sub-province is the spatial-compositional variation from South to North (Weigand and Ragland 1970; Cummins et al. 1992). The basaltic rocks can be subdivided into three principal groups: (1) olivine-normative, (2) high-TiO_2 quartz-normative, and (3) low-TiO_2 quartz-normative with a less common high-Fe_2O_3t quartz-normative type. The olivine-normative rocks predominate within the southern ENA (SENA), whereas the quartz-normative rocks are predominant in the northern ENA (NENA). The transition between the olivine-normative and the quartz-normative North occurs around Virginia–North Carolina (Weigand and Ragland 1970) although some olivine- or quartz-normative rocks are found outside their regions. The spatial-compositional variability is attributed to a number of processes including: mantle source (enriched subcontinental lithospheric mantle or mantle-plume), open- versus closed-system magmatism, depth and/or density-controlled partial melting and fracture-zone or transform fault influence (Weigand and Ragland 1970; Greenough and Hodych 1990; Cummins et al. 1992; Puffer 1992; Murphy et al. 2011; Callegaro et al. 2013, 2014; Merle et al. 2013; Whalen et al. 2015).

The North Mountain basalt (NMB) erupted within the Fundy Basin of the Northern Appalachians and is one of the best exposures of CAMP-related rocks in Eastern North America. The rocks are well studied and dated however unlike other regions of the CAMP the primary melt composition and thermal regime of the NMB has not been investigated. In this paper, we present new whole rock geochemical data from the North Mountain basalt. Samples were collected from surface exposures along the entire length of the formation as well as from a 160-m-deep drill well. We use the data to estimate the primary melt composition of the NMB and their mantle potential temperatures (T_P) in order to compare with basalt from other regions of the ENA sub-province and constrain the extent of mantle source heterogeneity between the SENA and NENA.

Geological background

The North Mountain basalts were emplaced in the Bay of Fundy graben, the most northerly of the sixteen basins of the Newark Supergroup (Schlische et al. 2002) that run parallel to the continental margin of the North America (Figs. 2, 3). The first descriptions of the North Mountain basalts were produced by Powers (1916), whereas Powers and Lane (1916) reported the evidence for differentiation in these basalts which were used by Bowen (1916) to document his model of differentiation in mafic magmas. Moreover, some of the basalt flows appear to have experienced silicate

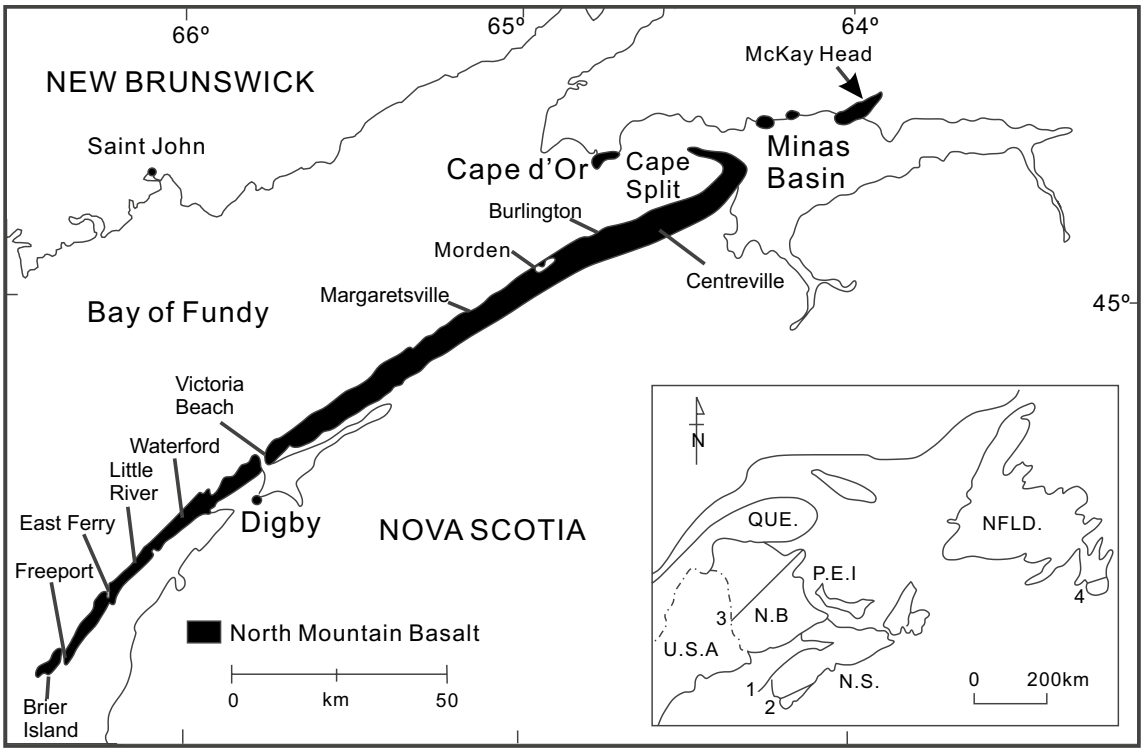

Fig. 2 Geological map of the North Mountain basalt and sampling locations. *Inset* map of Atlantic Canada showing the distribution of CAMP-related mafic volcanic and intrusive rocks. *1* North Mountain Basalt, *2* Shelburne Dyke, *3* Caraquet Dyke, *4* Avalon Dyke. Modified from Dostal and Greenough (1992)

liquid immiscibility (Greenough and Dostal 1992a; Shellnutt et al. 2013).

The NMB conformably overlies Early Mesozoic siltstones and shales (Blomidon Formation) and continental red conglomerates and sandstone (Wolfville Formation) of the Fundy Group. The Mesozoic strata lie unconformably on Carboniferous and older rocks. The basalts which were emplaced just above the Triassic–Jurassic boundary are unconformably overlain by lacustrine limestones and continental clastic sedimentary rocks (Olsen et al. 1987; Cirilli et al. 2009). The Mesozoic rocks of the Bay of Fundy form a large, asymmetrical, plunging syncline that dips more-steeply on the northern side. The northern boundary of the basin is delineated by a major south-dipping fault, which may represent the western extent of the boundary between the Meguma and Avalon terranes. Radiometric dating (U–Pb, $^{40}Ar/^{39}Ar$) of basalts yielded an age of 202 Ma (Hodych and Dunning 1992; Kontak and Archibald 2003) and Olsen et al. (1982, 1987) assigned them to the earliest Jurassic on the basis of stratigraphy and paleontology.

The basalts form a prominent cuesta which extends for about 200 km along the southern shore of the Bay of Fundy with correlative flows on the north shore of the Minas Basin and in Cape Breton Island (Greenough and Dostal 1992b; White et al. 2017). The basalts thin from southwest (~400 m thick) to the northwest (~275 m), probably underlie most of the Bay of Fundy and cover an area of about 10,000 km^2 (Dostal and Greenough 1992). The basalts underwent zeolite facies metamorphism (Aumento 1966), which modified the primary mineralogy of the middle unit. The altered rocks have high contents of LOI (up to >5 wt%). The alteration led to a redistribution of alkalis and Ca in some samples (Dostal and Dupuy 1984). In addition, Cu was also affected during metamorphism. Dostal and Dupuy (1984) documented that while this element is depleted in many samples, some altered basalts have rather high concentrations (>1000 ppm Cu).

Petrography

The basaltic formation includes three units. The lower and upper units are composed of thick medium- to coarse-grained massive flows, whereas the middle unit up to 50-m thick consists of a series of thin extensively altered amygdaloidal lava flows with abundant zeolites and quartz, which also fill abundant amygdules. The basalts of the lower and upper units are fresh and contain zoned microphenocrysts of plagioclase ($An_{60–80}$) and augite as well as minor Fe–Ti oxides set in a matrix composed of plagioclase, augite,

Fig. 3 Field photographs of the NMB. **a** Columnar joint structure of the upper flow (Long Island, near Tiverton). *The leftmost column* is ~9 m high (photo taken by D. Kontak). **b** Coastal exposure of the upper flow beneath the Margaretsville lighthouse. **c** North Mountain basalt overlying the Fundy Group (Triassic–Jurassic) sedimentary rocks of the Blomidon Formation at Five Islands Provincial Park (photo taken by D. Kontak). **d** Plan view of columnar joints along the shore line at Canada Creek. The *pen*, *near center of photo*, is ~15 cm in length. **e** Middle flow basalt with amygdules (*green*, *white*, *red*, *orange*), West of Harbourville. **f** Xenolith of middle flow basalt with amygdules within the upper flow (French Cross, Morden). The *pen* is the same in **d**

pigeonite, Fe–Ti oxides, accessory apatite, and devitrified glass. The NMB has long been known for its varied and abundant zeolite minerals. In fact, it hosts the type locality for the mordenite and a comprehensive summary of their occurrences was published nearly 100 years ago (Walker and Parsons 1922). However, the degree of zeolitization of the basalts is variable.

Sampling and analytical methods

A total of forty samples were collected for this study. The twenty-four samples (11,392 to 11,420) are specimens collected from outcrops of the basaltic belt (cuesta), in area between Centerville (near Kentville) and Brier Island whereas sixteen samples labeled 13 to 690 are the core samples from the diamond drill hole GVA-77-3 drilled ~1 km southwest from the village of Morden in the Annapolis Valley (Fig. 2). The numbers refer to the depth from the surface (in feet). The drill hole was described by Kontak et al. (2005). From the surface to the depth of about 520 feet, the rocks are from the middle unit which is composed of 15 flows each about 3–20 m thick. The samples numbered 537.5–690 are from the lower unit (Table 1).

Whole-rock abundances of major and some trace elements (Rb, Ba, Sr, Zr, Y, Ga, Cr, Ni, and V) were determined on glass disks and pressed pellets, respectively, using a Philips PW1400 X-ray fluorescence spectrometer at Saint Mary's University, Halifax (Dostal et al. 1994). The analytical uncertainties were estimated to be generally ~1% for the major elements and 5–15% for the trace elements. Rare earth and the other trace elements (Th, Nb, Hf) were determined by inductively coupled plasma-mass spectrometry (ICP-MS) at the Geoscience Laboratories of the Ontario Geological Survey. Precision and accuracy are given by Ayer and Davis (1997) and are generally within 5–10%. The full data suite is listed in Table 1.

Results

The North Mountain basalts are typically hypersthene-normative continental tholeiites with pigeonite in their mode (Fig. 4a, b). Overall, their composition resembles continental flood basalts from other continental flood basalt provinces and there does not appear to be significant compositional differences among the three units (upper, middle, lower) except for the extent of alteration (Dostal and Dupuy 1984; Dostal and Greenough 1992). The rocks from this study are similar to the basalt from the NENA in general and have trace element ratios indicative of an enriched mantle source that likely had a reducing relative oxidation state (Fig. 4c, d). The basalts display noticeable variations in major element compositions with Mg# (molar $Mg/Mg + Fe_{total}$) in our samples ranging from 0.68 to 0.34 and with MgO (wt%) from 9.5 to 3.7 indicating that many rocks experienced extensive fractional crystallization. The samples with the highest Mg# have the lowest incompatible trace element concentrations including Zr but the highest contents of pyroxene phenocrysts and Cr and Ni. The pegmatitic basalts have the lowest Mg# and MgO but high Zr (>150 ppm in Fig. 5).

On the primitive-mantle normalized trace element patterns, the North Mountain basalts exhibit shapes which are common in continental flood basalts. They display negative Ba, Nb, Sr, and Ti anomalies (Fig. 6a). The negative Ba and Sr anomalies are likely caused by fractional crystallization of plagioclase in the magma chamber or during magma ascent. The chondrite-normalized REE patterns (Fig. 6b) are subparallel, have moderately sloping with $(La/Yb)_n$ ~3–4, consistent with the low-pressure fractionation dominated by pyroxenes and plagioclase. The patterns do not have noticeable Eu anomalies despite the presence of plagioclase phenocrysts and Sr anomalies in the primitive mantle normalize plot.

Discussion

Petrogenesis of the North Mountain Basalt

Chemically, the NMB are typical continental tholeiitic basalts with characteristic Fe–Ti-enrichment fractionation trend and are comparable to the high-TiO_2 quartz normative type of Weigand and Ragland (1970). An increase of Fe, Ti, P, and V and decrease of Mg, Ca, Cr, and Ni with decreasing of Mg# but increase of Zr (taken in Fig. 4 as an index of fractionation in lieu of Mg# to avoid the alteration effect) is typical of tholeiitic fractionation trends pointing to crystallization of pyroxenes and plagioclase but a negligible fractionation effect of Fe–Ti oxides during the differentiation (Fig. 4b). The steeper decrease of Cr relative to Ni and Co in the basalts with higher Mg# suggests clinopyroxene crystallization but argue against significant olivine fractionation. However, the low contents of Ni in most samples imply a crystallization of olivine in a differentiation stage prior to eruption. Moreover, the slight increase of Al, Sr, and Al/Ca ratios in less fractionated basalts (<150 ppm Zr; Fig. 5) indicates a predominance of clinopyroxene over plagioclase during differentiation.

The variation of La/Yb versus Yb in basaltic rocks have been used to differentiate between compositional changes due to fractional crystallization, differences in degree of melting and source heterogeneity (Fan et al. 2008; Dostal et al. 2016). The La/Yb and Yb trend shown in Fig. 7 is

Table 1 Geochemical data of the North Mountain basalt

Sample	11392	11393	11394	11395	11396	11397	11398	11399
Location	Freeport	Freeport	Freeport	Freeport	Freeport	Freeport	Freeport	Freeport
Flow unit	Upper	Middle	Middle	Upper	Upper	Lower	Lower	Lower
SiO_2 (wt%)	52.00	49.60	51.60	51.40	52.20	52.10	51.90	51.20
TiO_2	0.92	1.25	0.98	0.96	0.93	1.34	1.19	0.95
$A1_2O_3$	12.20	13.40	12.80	12.40	12.60	13.90	13.00	12.60
Fe_2O_3t	10.40	11.50	11.20	10.60	10.70	12.10	11.30	12.20
MnO	0.18	0.16	0.20	0.18	0.19	0.18	0.17	0.16
MgO	7.83	7.55	8.49	8.64	8.47	5.88	6.99	8.90
CaO	10.70	6.15	10.80	10.60	11.00	10.00	10.50	12.30
Na_2O	1.76	4.15	1.84	1.73	1.95	2.41	1.84	1.77
K_2O	0.48	0.97	0.72	0.66	0.67	0.85	0.79	0.57
P_2O_5	0.12	0.16	0.12	0.12	0.12	0.17	0.15	0.12
LOI	1.80	4.90	1.40	1.40	1.15	1.30	1.30	0.90
Total	98.39	99.79	100.15	98.69	99.98	100.23	99.13	99.97
Mg#	59.9	56.5	60.0	61.7	61.1	49.0	55.1	63.3
Sc (ppm)	36	35	38	37	39	36	37	40
V	223	255	267	240	230	288	238	203
Cr	470	160	470	460	520	120	220	630
Co	36	36	36	35	38	39	38	36
Ni	98	61	101	99	107	52	67	95
Cu	117	50	70	36	13	66	176	109
Zn	76	80	83	76	76	95	90	69
Ga	16	18	17	16	17	20	18	19
Rb	15	26	25	24	17	29	28	20
Sr	187	436	171	162	168	193	179	155
Y	18	23	20	19	19	25	22	18
Zr	90	109	90	92	87	114	108	81
Nb	8	11	9	8	8	12	11	8
Ba	389	108	140	122	113	164	140	82
Hf	2.3	2.7	2.0	2.1	2.4	3.1	2.7	2.0
La	10.6	13.7	11.6	11.0	10.9	14.8	13.3	9.7
Ce	21.8	28.4	23.0	23.1	23.0	31.0	28.0	20.5
Pr	2.8	3.8	3.2	3.0	3.1	4.1	3.7	2.8
Nd	12.8	17.1	14.1	13.6	13.8	18.5	16.8	12.5
Sm	3.0	3.9	3.3	3.2	3.2	4.3	4.0	3.0
Eu	1.05	1.35	1.11	1.07	1.13	1.51	1.37	1.07
Gd	3.5	4.7	4.0	3.8	3.8	5.1	4.7	3.7
Tb	0.6	0.8	0.7	0.6	0.6	0.8	0.7	0.6
Dy	3.3	4.1	3.6	3.5	3.4	4.6	4.3	3.4
Ho	0.64	0.82	0.75	0.71	0.71	0.91	0.84	0.67
Er	1.9	2.3	2.1	2.1	2.0	2.7	2.5	1.9
Tm	0.3	0.3	0.3	0.3	0.3	0.4	0.4	0.3
Yb	1.7	2.1	2.0	1.9	1.9	2.4	2.3	1.8
Lu	0.27	0.33	0.30	0.30	0.30	0.36	0.33	0.28
Th	2.0	2.3	1.9	2.0	2.0	2.4	2.6	1.8

Table 1 (continued)

Sample	11401	11402	11403 Little	11404	11406	11407 Victoria	11408 Victoria	11409 Victoria
Location	East Ferry	East Ferry	River	Centreville	Waterford	Beach	Beach	Beach
Flow unit	Lower	Middle	Lower	Upper	Lower	Middle	Middle	Lower
SiO_2 (wt%)	51.40	51.70	51.60	51.10	50.50	52.40	51.80	51.70
TiO_2	1.28	0.94	0.89	0.94	1.10	1.71	1.01	1.03
$A1_2O_3$	13.30	12.60	12.30	12.50	12.20	13.00	13.00	13.00
Fe_2O_3t	11.90	10.40	10.40	10.70	10.60	13.30	10.80	9.57
MnO	0.21	0.18	0.17	0.20	0.20	0.18	0.18	0.14
MgO	5.94	8.40	9.18	8.89	8.21	4.66	8.39	8.49
CaO	8.93	10.50	12.10	11.20	10.90	8.76	11.60	11.70
Na_2O	2.59	2.18	1.65	1.62	1.70	2.27	1.67	1.71
K_2O	1.04	0.81	0.69	0.44	0.99	1.46	0.66	1.10
P_2O_5	0.16	0.12	0.11	0.12	0.14	0.21	0.13	0.13
LOI	1.90	1.45	1.00	2.05	1.95	1.55	0.90	1.20
Total	98.65	99.28	100.09	99.76	98.49	99.50	100.14	99.77
Mg#	49.7	61.5	63.6	62.2	60.5	41.0	60.6	63.7
Sc (ppm)	34	38	40	38	38	37	37	36
V	288	231	210	217	258	324	229	224
Cr	140	490	610	460	510	67	470	430
Co	36	36	38	38	41	39	38	34
Ni	51	102	103	106	93	38	95	91
Cu	50		72	47	34	180	93	71
Zn	99	73	76	97	112	74	72	80
Ga	19	16	15	16	16	21	17	17
Rb	29	25	24	12	18	28	20	18
Sr	196	163	155	187	175	190	170	175
Y	23	19	17	19	21	31	19	21
Zr	116	87	80	88	101	155	91	96
Nb	11	9	9	10	11	12	11	10
Ba	156	125	92	64	102	223	108	87
La	13.5	11.2	9.7	10.9	12.6	20.1	11.4	15.5
Ce	29.6	22.1	23.0	23.0	25.7	41.8	23.9	35.4
Pr	4.0	3.2	2.7	3.1	3.6	5.7	3.2	4.7
Nd	17.9	14.1	12.5	14.0	16.0	25.1	14.9	20.6
Sm	4.3	3.4	3.1	3.2	3.8	5.8	3.6	4.4
Eu	1.48	1.14	1.06	1.10	1.33	1.91	1.23	1.54
Gd	5.0	4.0	3.8	4.0	4.6	6.8	4.3	5.1
Tb	0.8	0.7	0.6	0.6	0.7	1.1	0.7	0.8
Dy	4.5	3.6	3.4	3.5	4.1	6.0	3.8	4.3
Ho	0.91	0.73	0.68	0.71	0.82	1.21	0.76	0.85
Er	2.6	2.1	2.0	2.1	2.3	3.4	2.1	2.4
Tm	0.4	0.3	0.3	0.3	0.3	0.5	0.3	0.4
Yb	2.4	1.9	1.8	2.0	3.1	2.0	2.0	2.1
Lu	0.37	0.30	0.28	0.31	0.32	0.47	0.31	0.32
Hf	3.1	2.2	1.7	1.7	2.4	3.7	1.7	2.1
Th	2.4	2.0	1.4	1.7	2.2	3.8	2.0	2.1

Table 1 (continued)

Sample	11410	11411	11412	11413	11417	11418	11419 Brier	11420 Brier
Location	Burlington	Burlington	Morden	Margaretsville	Digby	Brier Island	Island	Island
Flow unit	Lower	Lower	Upper	Upper	Upper	Lower	Upper	Upper
SiO_2 (wt%)	51.60	50.90	49.90	52.40	53.60	51.10	51.80	52.60
TiO_2	1.07	1.28	1.24	1.16	1.97	0.83	1.00	0.97
$A1_2O_3$	12.80	13.60	14.50	13.90	12.10	11.70	12.80	12.80
Fe_2O_3t	11.20	11.40	11.70	11.90	14.40	9.95	10.70	10.80
MnO	0.19	0.16	0.20	0.19	0.23	0.17	0.18	0.18
MgO	8.31	6.53	5.94	5.94	3.75	9.89	8.03	8.09
CaO	11.00	9.29	10.70	10.30	8.23	12.00	10.90	11.00
Na_2O	1.66	2.15	2.03	2.20	2.34	1.56	2.00	1.97
K_2O	0.78	0.92	0.46	1.17	1.22	0.50	0.72	0.61
P_2O_5	0.13	0.16	0.16	0.15	0.25	0.10	0.13	0.12
LOI	1.15	3.50	2.10	0.80	1.15	0.75	1.10	1.05
Total	99.89	99.89	98.93	100.11	99.24	98.55	99.36	100.19
Mg#	59.5	53.1	50.1	49.7	34.0	66.3	59.8	59.7
Sc (ppm)	36	34	35	35	37	41	39	39
V	272	284	309	267	358	239	233	234
Cr	380	120	110	160	37	690	440	430
Co	40	37	36	36	41	40	36	37
Ni	96	52	58	70	26	112	97	102
Cu	101	182	183	39	322	80	11	107
Zn	82	91	94	95	121	71	84	91
Ga	17	18	20	18	22	15	17	16
Rb	23	29	13	33	41	16	26	19
Sr	171	184	215	196	196	147	171	176
Y	20	23	26	23	38	16	20	20
Zr	96	114	126	111	188	73	92	92
Nb	11	12	12	10	17	8	9	11
Ba	129	158	81	141	250	65	130	102
La	12.0	14.4	17.0	14.8	25.7	9.0	12.7	11.6
Ce	25.2	30.2	34.7	30.6	53.8	19.2	26.3	24.2
Pr	3.4	4.1	4.7	4.1	7.2	2.6	3.6	3.3
Nd	15.4	18.3	20.8	18.3	31.7	11.90	16.1	14.4
Sm	3.7	4.2	4.7	4.2	7.4	3.0	3.8	3.4
Eu	1.3	1.46	1.6	1.45	2.24	1.06	1.29	1.14
Gd	4.4	5.1	5.5	5.0	8.9	3.6	4.5	4.1
Tb	0.7	0.8	0.9	0.8	1.4	0.6	0.8	0.7
Dy	4.0	4.5	4.9	4.5	7.6	3.4	4.1	4.0
Ho	0.78	0.90	1.01	0.91	1.52	0.67	0.82	0.82
Er	2.3	2.6	3.0	2.7	4.4	1.9	2.4	2.4
Tm	0.3	0.4	0.4	0.4	0.6	0.3	0.4	0.3
Yb	2.1	2.4	2.8	2.5	4.1	1.8	2.3	2.3
Lu	0.32	0.37	0.43	0.38	0.61	0.29	0.35	0.34
Hf	2.2	2.8	3.3	2.3	4.5	1.7	2.4	2.3
Th	2.1	2.4	3.1	2.1	4.2	1.3	2.1	2.0

Table 1 (continued)

Sample	13	22.5	40	59	114	165	263	344
Location	Morden	Morden	Morden	Morden	Morden	Morden	Morden	Morden
Rock unit	Middle	Middle	Middle	Middle	Middle	Middle	Middle	Middle
SiO_2 (wt%)	48.50	50.40	49.50	50.90	50.20	48.90	50.20	48.30
TiO_2	1.25	1.22	1.26	1.27	1.17	1.22	1.22	1.24
$A1_2O_3$	13.80	13.60	13.60	14.00	13.40	13.90	13.50	13.70
Fe_2O_3t	11.70	11.60	11.80	11.90	11.20	11.50	10.80	11.40
MnO	0.18	0.18	0.17	0.20	0.17	0.18	0.24	0.18
MgO	5.59	5.65	6.04	6.31	5.93	6.11	6.43	6.16
CaO	9.69	9.13	10.70	10.70	9.45	10.20	9.27	10.20
Na_2O	2.34	2.57	1.95	2.12	2.67	2.30	3.05	2.28
K_2O	0.70	1.28	0.95	0.69	0.55	0.71	0.77	0.65
P_2O_5	0.16	0.16	0.16	0.16	0.15	0.16	0.16	0.16
LOI	5.50	2.90	2.80	1.35	5.15	4.75	2.55	4.40
Total	99.41	98.69	98.93	99.60	100.04	99.93	98.19	98.67
Mg#	48.6	49.1	50.3	51.2	51.2	51.3	54.1	51.7
Sc (ppm)	34	33	62	19	33	32	34	34
V	209	273	256	292	225	260	269	233
Cr	97	91	120	120	110	120	140	150
Co	38	34	69	21	36	34	36	36
Ni	50	48	100	30	54	51	61	56
Cu	81	253	170	16	104	23	91	21
Zn	105	92	159	75	88	80	107	93
Ga	20	19	34	10	17	18	18	20
Rb	39	63	23	37	28	33	31	38
Sr	314	266	327	101	217	179	163	184
Y	25	23	44	13	21	21	23	23
Zr	111	109	120	113	101	117	109	114
Nb	22	19	28	30	23	29	22	22
Ba	142	154	128	106	152	102	68	103
La	15.1	13.8	26.8	7.6	13.4	13.4	13.6	14.5
Ce	31.7	29.3	56.7	15.9	28.3	28.7	28.5	30.6
Pr	4.2	3.9	7.5	2.1	3.8	3.8	3.8	4.1
Nd	18.7	17.4	33.4	9.3	17.0	17.0	16.4	18.1
Sm	4.4	4.1	7.8	2.1	4.0	4.0	4.0	4.3
Eu	1.53	1.39	2.61	0.76	1.33	1.35	1.41	1.43
Gd	5.2	4.8	9.4	2.7	4.7	4.7	4.8	5.2
Tb	0.8	0.8	1.5	0.4	0.8	0.8	0.8	0.8
Dy	5.0	4.7	9.0	2.6	4.6	4.6	4.7	4.8
Ho	1.01	0.95	1.80	0.52	0.92	0.92	0.94	0.98
Er	2.9	2.7	5.2	1.5	2.7	2.7	2.7	2.8
Tm	0.4	0.4	0.7	0.2	0.4	0.4	0.4	0.4
Yb	2.7	2.5	4.8	1.4	2.4	2.4	2.5	2.7
Lu	0.43	0.39	0.73	0.21	0.38	0.39	0.38	0.40
Hf	2.9	2.3	3.2	2.1	2.6	2.8	2.9	3.3
Th	2.9	2.6	2.7	2.3	2.4	2.5	2.5	2.5

Table 1 (continued)

Sample	390	418	514	537.5	591.5	619.5	678	690
Location	Morden	Morden	Morden	Morden	Morden	Morden	Morden	Morden
Rock unit	Middle	Middle	Middle	Lower	Lower	Lower	Lower	Lower
SiO_2 (wt%)	49.50	47.30	48.60	49.80	51.00	51.20	51.00	47.70
TiO_2	1.25	1.24	1.25	1.19	1.26	1.09	1.18	1.32
$A1_2O_3$	13.40	13.60	14.40	14.20	13.80	13.20	14.40	14.90
Fe_2O_3t	11.50	11.70	10.80	10.40	11.80	11.20	8.92	9.24
MnO	0.16	0.17	0.14	0.12	0.23	0.20	0.11	0.08
MgO	5.80	6.72	6.35	6.95	6.39	8.08	8.30	9.49
CaO	9.33	9.89	7.52	9.87	10.70	10.80	9.65	7.36
Na_2O	2.67	2.33	4.49	1.98	2.14	1.76	2.14	2.53
K_2O	0.93	0.41	0.63	0.52	0.32	0.86	0.54	0.65
P_2O_5	0.16	0.16	0.16	0.15	0.16	0.14	0.13	0.16
LOI	4.15	6.60	5.30	4.10	1.30	1.10	3.70	5.90
Total	98.85	100.12	99.64	99.28	99.10	99.63	100.07	99.33
Mg#	50.0	53.2	53.8	57.0	51.7	58.8	64.8	67.0
Sc (ppm)	34	34	31	33	35	35	37	36
V	256	293	226	234	258	272	230	315
Cr	120	120	75	89	110	270	200	130
Co	37	39	32	33	37	40	28	26
Ni	56	62	51	52	54	89	65	54
Cu	79	38	29	227	138	147	63	116
Zn	89	101	65	53	111	92	64	87
Ga	17	19	19	19	19	17	20	19
Rb	20	33	29	14	16	26	12	21
Sr	196	195	197	189	209	183	230	259
Y	24	23	22	22	24	20	21	21
Zr	122	109	130	104	103	96	97	105
Nb	19	20	23	23	14			26
Ba	172	66	110	92	111	138	129	292
La	15.2	13.8	14.8	13.2	15.0	12.8	11.1	13.9
Ce	31.7	29.9	29.4	29.0	31.8	26.3	22.1	29.1
Pr	4.2	4.0	3.9	4.0	4.3	3.5	2.9	3.9
Nd	18.7	18.0	17.3	17.7	19.0	15.3	13.0	17.1
Sm	4.4	4.4	4.2	4.2	4.4	3.8	3.5	4.0
Eu	1.51	1.47	1.40	1.43	1.57	1.32	1.47	1.54
Gd	5.3	5.1	4.9	4.9	5.3	4.4	4.5	5.0
Tb	0.9	0.8	0.8	0.8	0.9	0.7	0.7	0.8
Dy	5.2	5.0	4.8	4.8	5.2	4.4	4.4	4.7
Ho	1.01	1.01	0.95	0.97	1.05	0.88	0.90	0.93
Er	2.9	2.8	2.8	2.8	3.0	2.5	2.6	2.6
Tm	0.4	0.4	0.4	0.4	0.4	0.4	0.4	0.4
Yb	2.8	2.7	2.6	2.5	2.8	2.3	2.6	2.5
Lu	0.42	0.41	0.39	0.40	0.44	0.35	0.41	0.39
Hf	3.0	2.7	2.6	2.5	2.7	2.3	2.4	2.7
Th	2.8	2.5	2.3	2.2	2.7	2.1	2.4	2.5

t total Fe expressed as Fe_2O_3, *LOI* loss on ignition, *Mg#* $(Mg/(Mg + Fe_{total}) \times 100$

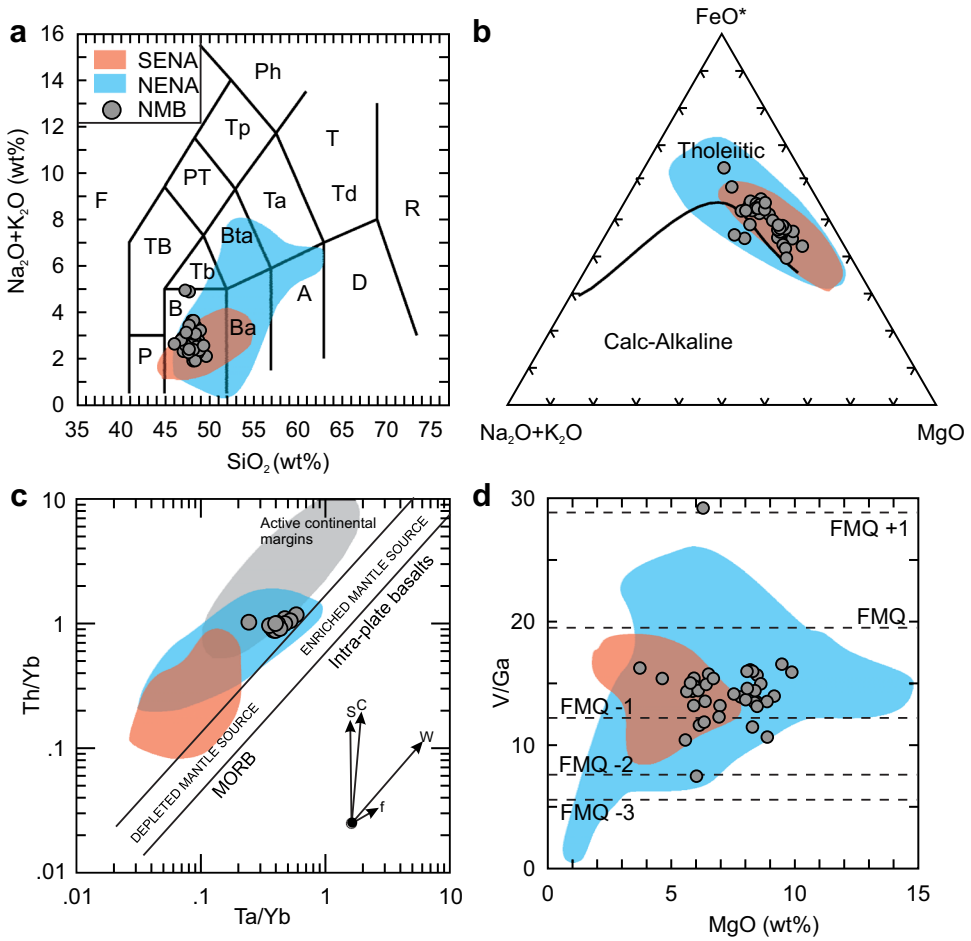

Fig. 4 **a** $Na_2O + K_2O$ (wt%) versus SiO_2 (wt%) chemical classification of volcanic from the ENA sub-province of the CAMP and the North Mountain basalt. *F* foidite, *P* picro-basalt, *B* basalt, *Ba* basaltic andesite, *A* andesite, *D* dacite, *R* rhyolite, *Td* trachydacite, *T* trachyte, *Ta* trachyandesite, *Bta* basaltic trachyandesite, *Tb* trachybasalt, *TB* tephorite or basanite, *PT* phono-tephrite, *Tp* tephriphonolite, *Ph* phonolite. **b** A ($Na_2O + K_2O$ wt%)–F (FeOt wt%)–M (MgO wt%) diagram showing the tholeiitic trend of the ENA basalt and North Mountain basalt. **c** Th/Yb versus Ta/Yb basalt discrimination diagram of Wilson (1989) showing the differences between subduction and oceanic basalts derived from depleted and enriched source. *Vectors* show influence of each component, *S* subduction component, *C* crustal component, *W* within plate enrichment, *f* fractional crystallization. **d** *Diagram* indicating the redox state of the ENA basalt and North Mountain basalt using the bulk-rock V/Ga ratio. Reference lines at various fO_2 are after Mallmann and O'Neill (2009). ENA data from Chowns and Williams (1983), Grossman et al. (1991), Pe-Piper and Reynolds (2000)

consistent with fractional crystallization (horizontal trend) and argues against large-scale source heterogeneity in the ENA basalts, although some NENA basalts follow the source heterogeneity trend. Several incompatible element ratios are sensitive to melting conditions such as pressure or depth of melting. The Dy/Yb versus Zr plot (Fig. 5f) suggests that all parent melts were generated at about the same depth in the spinel peridotite stability field (60–70 km depth).

The elevated Th/La ratios are commonly used as indices to identify crustal contamination (Jochum et al. 1991; Dostal et al. 2016). Constant Th/La ratios with Zr (Fig. 5e) suggest that there was no significant shallow-seated crustal contamination of the basalts, although relatively high values (0.15–0.20) compared to the mantle values (0.12—Sun and McDonough 1989) indicate that the parent magma was either contaminated prior to emplacement or that it was derived from subduction modified mantle. Murphy et al. (2011) inferred from Nd isotope systematics that the parent magma was derived from a subcontinental lithospheric mantle.

Thermal regime of the ENA sub-province

Primary melt compositions and mantle potential temperature estimates (T_P) were calculated for the North Mountain basalt using PRIMELT3 (Table 2). Previous T_P calculations of the ENA basalts relied on the older versions of PRIMELT; however, there are significant improvements to the software including correcting better melt fractions, identifying the residuum mineralogy, and improved uncertainty

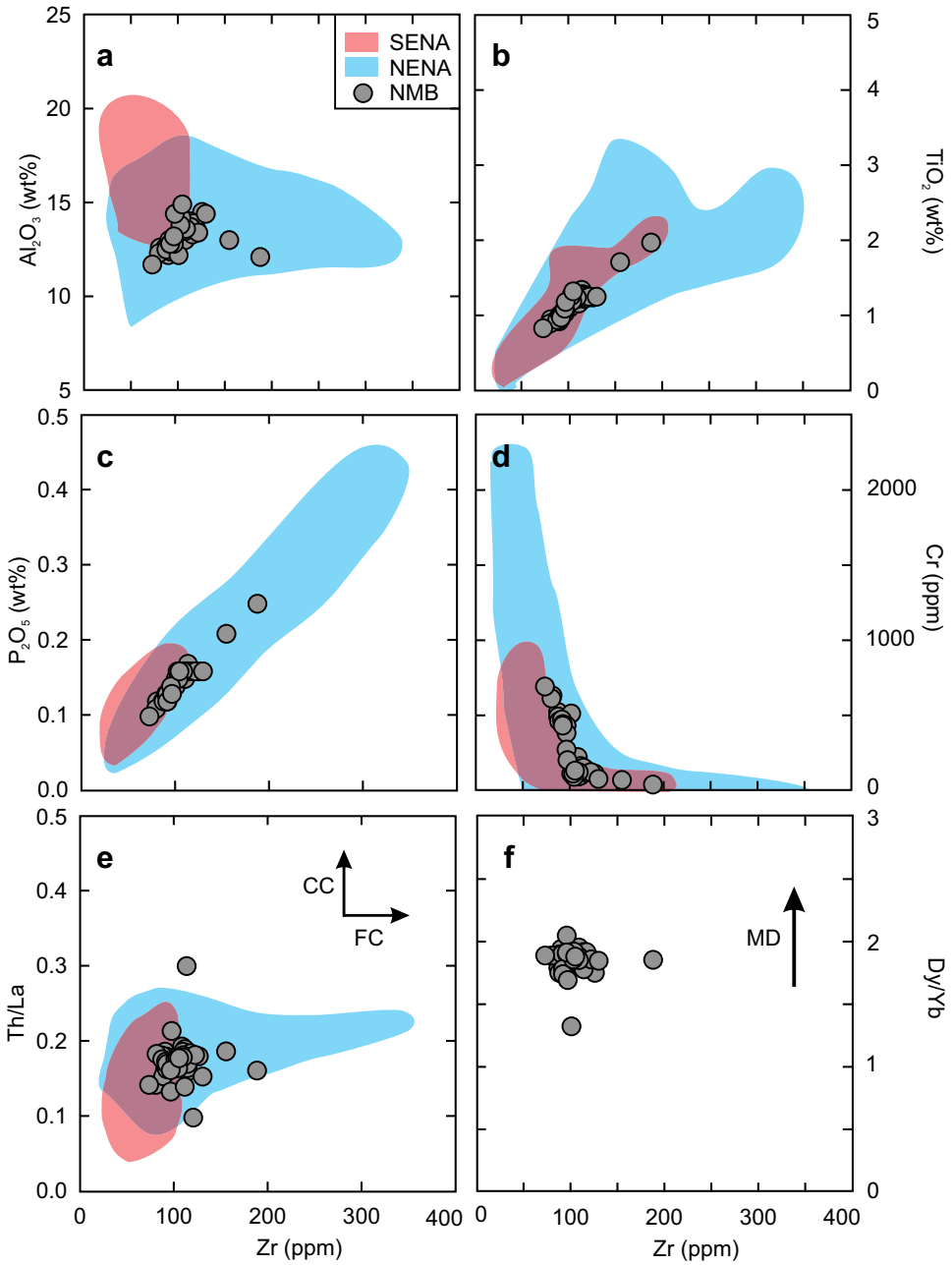

Fig. 5 Plots of Zr (ppm) versus **a** Al_2O_3 (wt%), **b** TiO_2 (wt%), **c** P_2O_5 (wt%), **d** Cr (ppm), **e** Th/La, and **f** Dy/Yb of the ENA basalt and North Mountain basalt. The Th/La plot depicts the vectors of crustal contamination and the Dy/Yb plot depicts the vectors of melting depth. ENA data from Chowns and Williams (1983), Grossman et al. (1991), Pe-Piper and Reynolds (2000). *CC* crustal contamination, *FC* fractional crystallization, *MD* melting depth

in the thermal estimates (Herzberg and Asimow 2015). The dry peridotite source MgO contents were set at 38.12 wt%, whereas the bulk FeOt of the source was set to the lowest possible values (8.57–8.69 wt%) that would produce meaningful (no augite fractionation warning) results. The modeled FeO was calculated by setting $Fe_2O_3 = 0.5 \times TiO_2$ to reflect a reducing relative (FMQ < 0) oxidation state (Fig. 4d). The accumulated fractional melt (AFM) results from PRIMELT3 are plotted on a series of FeOt versus MgO diagrams that show the primary melt composition and the equilibrium melting olivine control line (Fig. 8a, b). The solidus, melt fraction, and pressure lines shown in the models are derived from Herzberg and O'Hara (2002), Herzberg et al. (2007), and Herzberg and Asimow (2008, 2015). The primary melt compositions and olivine control lines for the North Mountain basalt are shown in Fig. 8a. According to the classification of Le Bas (2000), the calculated primary magma compositions are picritic (MgO = 14.9–16.6 wt%) and experienced ~11.5 to ~20.9% olivine loss (Table 2). The calculated initial olivine has a forsterite value of 90 and the melt fraction (amount of melting from the source) for all samples falls within a narrow (0.30–0.32) range (Fig. 8b).

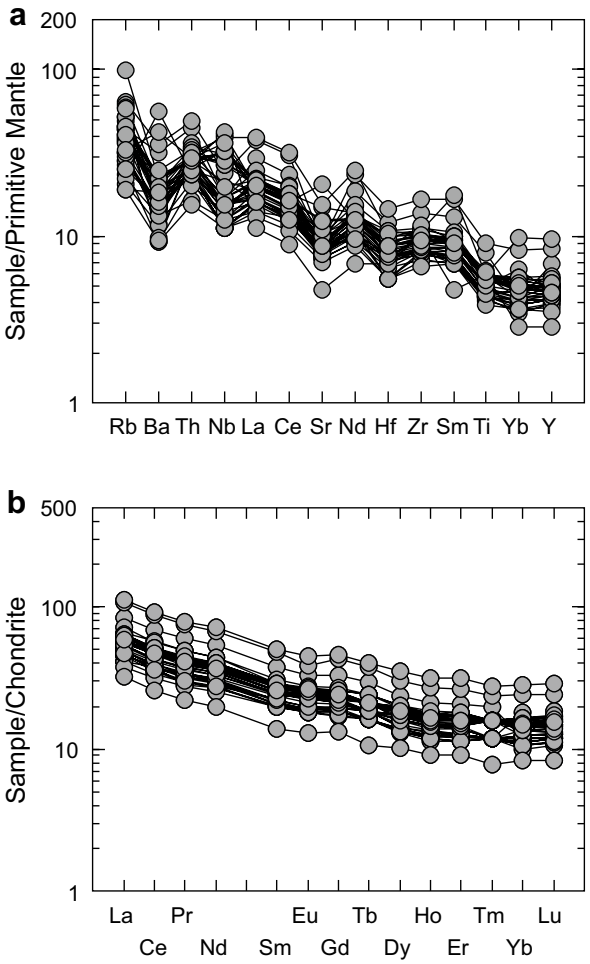

Fig. 6 **a** Primitive mantle normalized incompatible element and **b** chondrite-normalized rare-earth element plots of the North Mountain basalt. Normalizing values of Sun and McDonough (1989)

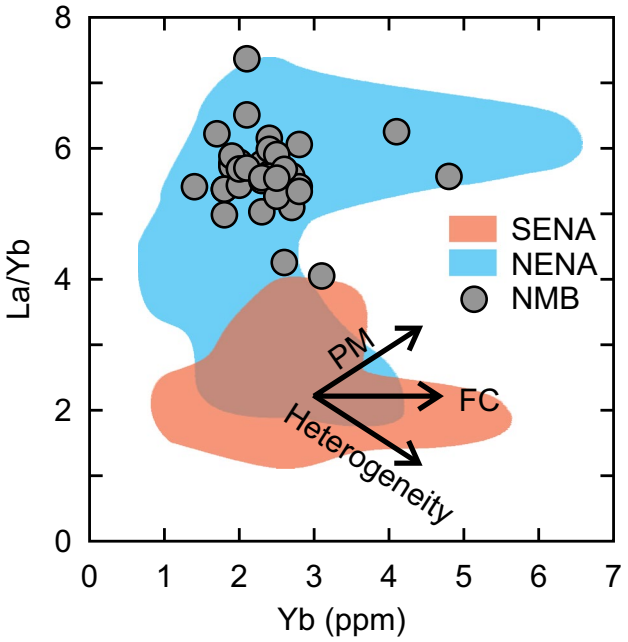

Fig. 7 La/Yb versus Yb (ppm) variation diagram for North Mountain basalts and the ENA. Vectors for fractional crystallization (FC), increase of the degree of melting, and source heterogeneity are after He et al. (2010). *PM* partial melting and heterogeneity = source heterogeneity. ENA data from Chowns and Williams (1983), Grossman et al. (1991), Pe-Piper and Reynolds (2000)

The eruptive temperatures (T) and mantle potential temperatures (T_P) are estimated to be 1330–1370 and 1430–1480 °C, respectively.

The mantle potential temperature estimates of the North Mountain basalt (T_P = 1430–1480 °C) are within the range reported by Hole (2015) and Callegaro et al. (2013) for selected rocks from the Central Atlantic Magmatic Province (Virginia, Georgia, South Carolina, North Carolina and Iberia) in general (T_P = 1450 ± 50 °C). A more thorough investigation of T_P of basaltic rocks from Georgia, North Carolina, Pennsylvania, New Jersey, and Newfoundland shows that there is no significant difference (T_{Psouth} = 1330–1490 °C; T_{Pnorth} = 1390–1490 °C) along the length of ENA subprovince (Fig. 9a). Overall, the T_P values of the CAMP are within or higher than ambient mantle (1300–1400 °C) but lower than temperatures expected from an anomalously (>1550 °C) hot mantle (Fig. 9a). Consequently, based on a limited dataset, Hole (2015) suggested that the T_P values of the CAMP are due to mantle insulation by the continental lithosphere rather than a mantle plume, a viewed shared by Coltice et al. (2007), Callegaro et al. (2013), and Whalen et al. (2015). Furthermore, the similar T_P values from South to North favor a thermal regime expected for a passive extensional (plate stress) model because a mantle-plume thermal regime is thought to change from the center to the margins (Herzberg and Gazel 2009). The fact that the basalts distal (~3000 km) from the inferred center of the CAMP have similar T_P as the basalts more proximal (<1000 km) to the center implies a consistent ambient thermal regime in each basin.

Compositional variability of the ENA mantle source

The accumulated fractional melting (AFM) primary melt compositions of this study show that the primary melt compositions from Northern Appalachians require an Fe-rich ($FeOt_{average}$ ≈ 8.6 wt %) mantle source and have a harzburgite residue (olivine + opx ± Cr-spinel), whereas basalt from the Southern Appalachians requires a less Fe-rich ($FeOt_{average}$ ≈ 8.3 wt%) mantle source composition where nearly two-thirds of the primitive melts have a spinel peridotite (olivine + opx + cpx + spinel-Al or Cr) residue and the rest indicate the primitive melts were in equilibrium with a garnet peridotite or harzburgite source (Fig. 9b).

Table 2 Primary melt compositions and mantle potential temperatures of North Mountain

Sample	11399	AFM	11403	AFM	11409	AFM	11418	AFM	NMB-8	AFM	NMB-19A	AFM
SiO_2 (wt%)	51.50	50.27	51.60	50.33	51.70	50.93	51.10	50.99	51.27	51.65	51.30	51.70
TiO_2	0.95	0.80	0.89	0.74	1.03	0.89	0.83	0.74	0.75	0.69	0.74	0.69
Al_2O_3	12.60	10.49	12.30	10.20	13.00	11.19	11.70	10.35	11.32	10.40	11.60	10.71
Fe_2O_3	10.20	0.40	10.40	0.37	9.57	0.44	9.95	0.36	9.77	0.34	9.62	0.34
FeO		9.36		9.54		8.82		9.17		8.99		8.85
FeOt	9.18		9.36		8.61		8.95		8.79		8.66	
MnO	0.16	0.16	0.17	0.17	0.14	0.14	0.17	0.18	0.16	0.17	0.16	0.17
MgO	8.90	16.22	9.18	16.56	8.49	14.94	9.89	15.67	10.60	15.20	10.47	14.87
CaO	12.30	10.27	12.10	10.08	11.70	10.11	12.00	10.64	11.87	10.93	11.74	10.86
Na_2O	1.77	1.47	1.65	1.36	1.71	1.47	1.56	1.38	1.26	1.16	1.13	1.04
K_2O	0.57	0.47	0.69	0.57	1.10	0.95	0.50	0.44	0.43	0.40	0.76	0.70
P_2O_5	0.12	0.10	0.11	0.09	0.13	0.11	0.10	0.09	0.08	0.07	0.07	0.06
LOI	0.90		1.00		1.20		0.75		1.0		1.20	
Pressure (bars)		1		1		1		1		1		1
FeO (source)		8.57		8.63		8.58		8.63		8.68		8.69
MgO (source)		38.12		38.12		38.12		38.12		38.12		38.12
Fe_2O_3/TiO_2		0.5		0.5		0.5		0.5		0.5		0.5
% ol addition		20.6		20.9		17.6		15.7		12.2		11.6
Melt fraction		0.306		0.317		0.302		0.311		0.317		0.316
Temperature (°C)		1360		1370		1340		1350		1340		1330
T_P (°C)		1470		1480		1430		1450		1440		1430

FeOt = Fe_2O_3t × 0.8998. The model compositions are normalized to 100% for the PRIMELT3 calculation

The implication is that the Northern basalts may be derived from an 'Fe-rich' mantle source and that the primary melts were in equilibrium with a harzburgitic residue although the original source may have been a spinel peridotite or a garnet peridotite (Herzberg and Asimow 2015). In contrast, southern basalts may be derived from a mantle source that was less 'Fe-rich' but that the residual lithology is typically spinel peridotite and thus the source was likely a spinel-bearing peridotite for most of the SENA basalt but in a few cases may have been a garnet-bearing peridotite.

Compositional variation of the ENA basalt

If the ENA basalts are related to mantle insulation (mantle global warming) and passive extension then the spatial-compositional variation observed from South to North must be related to inherent differences in the mantle sources that are beneath the Southern and Northern Appalachians (Weigand and Ragland 1970; Pegram 1990; Grossman et al. 1991; Puffer 2001; Marzoli et al. 2011; Murphy et al. 2011; Callegaro et al. 2013; Merle et al. 2013; Whalen et al. 2015). Most of the Triassic–Jurassic basins in the Northern Appalachians formed within the West Avalonia terrane, whereas the Triassic–Jurassic basins in Southern Appalachians (North Carolina to Florida) were formed within Carolinia or the Suwannee terrane (Dennis and Shervais 1996; Dennis and Wright 1997; Heatherington and Mueller 1999, 2003; Murphy and Nance 2002; Murphy et al. 2011; Callegaro et al. 2013). Crustal contamination and/or post-eruption hydrothermal alteration likely played a role during the ascent of the magmas through the crust before eruption but these processes are probably not responsible for the distinct regional chemical variation as they are highly localized and are unlikely to be uniform from region to region (Pegram 1990; Callegaro et al. 2013; Merle et al. 2013; Whalen et al. 2015).

The Sr–Nd–Pb isotopes across the ENA do not show systematic variation although the basaltic rocks from South Carolina and North Carolina have the lowest $^{87}Sr/^{86}Sr_i$ values (0.7045–0.7055), highest $\varepsilon_{Nd}(t)$ values ($\varepsilon_{Nd}(t) = +1$ to $+4$) and lowest Pb ($^{207}Pb/^{204}Pb = 15.60–15.53$; $^{208}Pb/^{204}Pb = 37.8–37.3$; $^{206}Pb/^{204}Pb = 18.0–17.5$) isotopic signatures (Merle et al. 2013; Callegaro et al. 2013). Callegaro et al. (2013) suggest that a maximum of ~10% recycled crust could explain the trace elemental and isotopic variability within the southern basalt and that the underlying mantle may be exceptional with respect to the rest of the CAMP. It is suggested that the subduction of upper continental crust (oceanic sediments) during the Paleozoic (Acadian Orogeny)

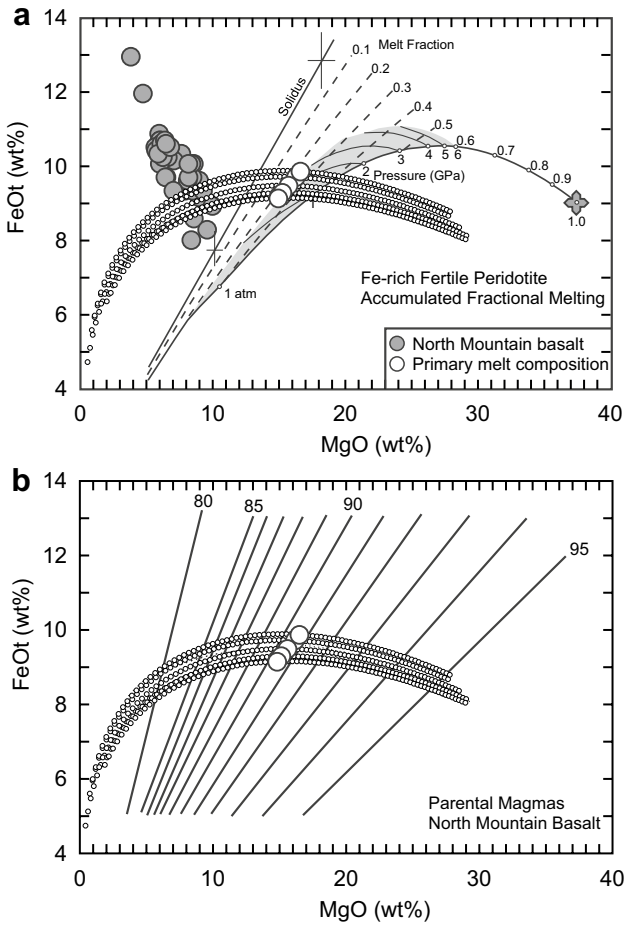

Fig. 8 **a** FeOt versus MgO of calculated primary melt compositions of the North Mountain basalt. The primary melt composition (*solid circles*) calculation results using PRIMELT3 (Herzberg and Asimow 2015). The *small white circles* represent the olivine control lines generated by the addition or subtraction of calculated equilibrium olivine compositions of the NMB. *Dashed lines* are melt fraction contours and the crosses indicate uncertainties in calculated FeO and MgO content related to $\pm 1\sigma$ $K_D^{Ol/L}{}_{FeO/MgO}$. **b** The primary melt compositions are plotted relative to the equilibrium olivine composition. The *numbers* (80, 85, 90, 95) represent Mg# (forsterite content) of olivine

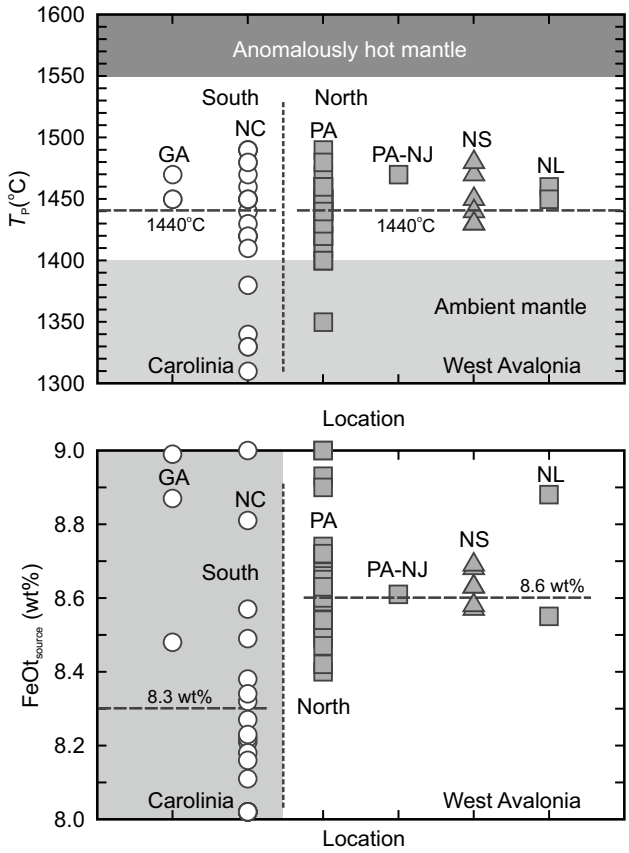

Fig. 9 **a** Mantle potential temperature (T_P) estimates of basalts from the ENA sub-province relative to ambient mantle (1300–1400 °C) and hot mantle associated with mantle-plumes (>1550 °C). The average T_P for the Southern and Northern Appalachians is 1440 °C. **b** Regional variability of the bulk FeOt content of the source required to produce a meaningful T_P result. *GA* South Georgia basin, Georgia; *NC* Deep River basin (Durham sub-basin), North Carolina; *PA* = Gettysburg basin, Pennsylvania; *PA-NJ* West Newark basin, Pennsylvania-New Jersey; *NS* Fundy basin, Nova Scotia; *NL* Avalon Peninsula, Newfoundland (Chowns and Williams 1983; Grossman et al. 1991; Pe-Piper and Reynolds 2000; Herzberg and Asimow 2008)

and possibly delaminated lower crust were incorporated or reacted with the ambient shallow lhzerolitic mantle. Trace elemental modeling shows that the range of La/Yb_N ratio of the rocks from the Southern ENA can be derived by ~15 to ~25% partial melting of 5% spinel peridotite source with a starting composition similar to primitive mantle (Fig. 10). The moderately high amount of partial melting is supported by the generally higher Mg# (60–72) and Ni (88–390 ppm) concentration in the basalts from the Southern Appalachians. Moreover, the calculated melt fraction for the primary melt compositions is consistent with the trace element models and range from 6.3 to 28.2% with an average of 16.9% (Table S1). Although it is likely that the mantle source of the SENA basalt was affected by subduction-related processes (Pegram 1990; Heatherington and Mueller 1999, 2003; Callegaro et al. 2013), our trace elemental modeling indicates that the mantle source of the southern Appalachians

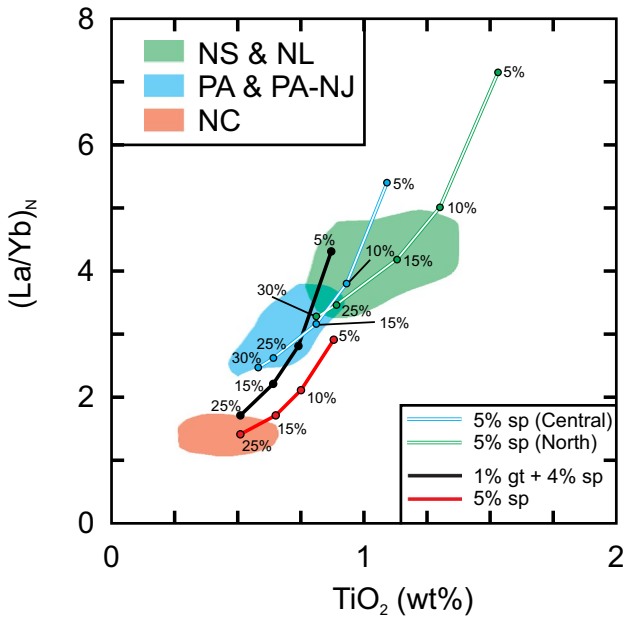

Fig. 10 The chondrite-normalized $(La/Yb)_N$ ratio versus TiO_2 (wt%) of ENA basalts from the Deep River basin (NC), Gettysburg basin, (PA), West Newark basin (PA-NJ), Fundy basin (NS) and Avalon Peninsula (NL). The *red* and *black model curves* are based on partial melting of a 5% spinel bearing peridotite (olivine = 52%, opx = 25%, cpx = 18%) and a peridotite with 1% garnet and 4% spinel (olivine = 52%, opx = 25%, cpx = 18%). Starting composition is equal to primitive mantle values of McDonough and Sun (1995). The *green* and *blue model curves* are based on a partial melting of a 5% spinel bearing peridotite (olivine = 52%, opx = 25%, cpx = 18%) assuming different 'mantle wedge' compositions for the north and central Appalachians (Table 3). Batch melting equation: $C_L/C_o = 1/D(1 - F) + F$, C_L concentration in the liquid, C_o original rock composition, D bulk distribution coefficient, F weight fraction of melt produced. K_d values: Ti, olivine = 0.04, opx = 0.1, cpx = 0.78, spinel = 0.048, garnet = 0.28; La, olivine = 0.007, opx = 0.0003, cpx = 0.056, spinel = 0.01, garnet = 0.001; Yb, olivine = 0.049, opx = 0.227, cpx = 0.28, spinel = 0.01, garnet = 8.5 (Arth 1976; Irving and Frey 1978; Fujimaki et al. 1984; Green et al. 1989, 2000; McKenzie and O'Nions 1991; Beattie 1994; Jenner et al. 1994; Johnson 1994; Salters and Longhi 1999; Klemme et al. 2006). The *triangles* are outliers from the Fundy Basin (NS)

may have had a trace element signature similar to primitive mantle.

Compared to the southern ENA basalt, the basalt from the northern ENA appears to have a relatively complicated petrogenetic history (Whalen et al. 2015). A similar but slightly different interpretation is expressed for the northern basaltic rocks as it is thought that a greater number of accretionary events or metasomatic events by subducted sediments affected the sub-Avalonia lithospheric mantle during the Paleozoic and yielded different 'subduction-related' signatures (Pegram 1990; Murphy et al. 2011; Merle et al. 2013; Whalen et al. 2015). Therefore, the major and trace elemental signatures are probably representative of the source region rather than syn-magmatic or post-magmatic processes (e.g., crustal contamination). A spinel peridotite source with a primitive mantle composition is unlikely to be responsible for the $(La/Yb)_N$ ratios observed in the northern ENA basalts as the melt curves cannot reproduce the high (>3) values or high TiO_2 content of the NMB or the Avalon dykes in Newfoundland (Fig. 10). The addition of a small amount of garnet to the mantle composition shifts the partial melting line upward and shows that lower amounts (5–15%) of partial melting can produce the compositional range of the basalts from the West Newark, Gettysburg, and Fundy basins and the dykes from the Avalon Peninsula but the PRIMELT3 calculations indicate that the primary melt compositions of the northern basalts were derived by high (~30%) melt fractions (Fig. 8a). The high melt fractions and low (≈10%) olivine loss in some of the models (NMB-8 and NMB-19A) would likely produce Ni-rich (>100 ppm) and high-MgO (>8 wt%) basalt. The MgO content for basalt that produced meaningful primary melt compositions typically have high MgO (>8 wt%) concentrations. However, the basalts from the northernmost (Nova Scotia and Newfoundland) ENA have lower Ni concentration (≤110 ppm) than the SENA (Ni = 88–390 ppm) but the basalts from Pennsylvania and New Jersey have Ni contents (Ni = 75–240 ppm) between the northernmost and southernmost. The 'transitional' composition of the basalts from the West Newark and Gettysburg basins also is reflected in their La/Yb_N ratios and TiO_2 (wt%) content (Fig. 10).

The calculated melt fraction, trace element modeling, and bulk Ni and TiO_2 contents are at odds suggesting that the mantle source of the NENA basalt must be different than the SENA. Mantle metasomatism is likely responsible for enrichment of some major and trace (K, Fe, Ca, Ti, Nb, and Ta) elements and isotopes that may be related to recent or even ancient events (Menzies et al. 1983; Dawson 2002; Ionov et al. 2002; O'Reilly and Griffin 2013). Mantle xenolith compositions reported from the Trans-Mexican Volcanic Belt (TMVB), considered indicative of a mantle-wedge source, show variability and trace element enrichment relative to primitive mantle (Mukasa et al. 2007). If a mantle xenolith (X-30 from Mukasa et al. 2007) composition from the TMVB is used as a proxy for the type of mantle that was present during the Early Jurassic beneath the North Appalachians then it appears that the high melt fractions and trace element modeling can be reconciled. The batch melting curve (green line) for the 'mantle wedge' peridotite is shown

in Fig. 10. A small amount of melting (<10%) produces the high La/Yb_N ratios (>5) but larger amounts of melting (>15%) produce the range (La/Yb_N = 3–4) of observed values in the rocks from Newfoundland (Avalon Peninsula) and Nova Scotia (Fundy Basin). The TiO_2 concentration was not reported by Mukasa et al. (2007) but we use a value of ~0.35 wt% which is high but lower than metasomatized spinel peridodite xenoliths (TiO_2 ≤0.46 wt%) from southeastern Mongolia (McDonough 1990; Kononova et al., 2002). The model is in agreement with the calculated melt fraction (20–30%) but the mantle xenolith composition cannot, within reason, reproduce the lower La/Yb_N (<3) and TiO_2 values of the basalt from the West Newark and Gettysburg Basins.

The basalts from the Mid-Atlantic States (New Jersey, Pennsylvania) are referred to as having a 'transitional' composition between the SENA and NENA basalts (Marzoli et al. 2011; Merle et al. 2013; Whalen et al. 2015). Although the 'transitional' basalts are still derived from a metasomatized mantle source, the amount of influence from subduction that the source experienced is thought to be different and contributed to their slightly different compositions as compared with the North Mountain basalt (Whalen et al. 2015). The differences in the structural controls related to subduction between the northern basalts and the transitional basalt could be the explanation for their different TiO_2 and La/Yb_N ratios in Fig. 10 and why the 'proxy mantle wedge' source composition cannot reproduce the values from the West Newark and Gettysburg Basins. If we use a mantle source composition (Table 3) that is 'transitional' between SENA and NENA rocks then values similar to the range observed in the West Newark and Gettysburg Basins can be reproduced and consistent with the PRIMELT3 melt fraction calculation (>25% melting).

Variability in mantle source composition between the basalt of the SENA and NENA is largely attributed to differences in the precise processes that occurred during Paleozoic subduction and accretion of West Avalonia and Carolinia to eastern North American margin (Puffer 2001; Murphy et al. 2011; Callegaro et al. 2013; Merle et al. 2013; Whalen et al. 2015). However, there may be an additional reason for the chemical differences between the regions of the NENA. Wide spread Late Devonian silicic plutonism is a defining difference between the tectonic evolution of the Northern and Southern Appalachians (Murphy et al. 1999; Dorais and Paige 2000; Dorais 2003; Tomascak et al. 2005; Shellnutt and Dostal 2015). The plutonism is spatially restricted to the regions north of New Hampshire and Vermont but is concentrated in Maine, New Brunswick, and Nova Scotia (Murphy et al. 1999). Shortly after the emplacement of the batholiths, there was a significant eruption of TiO_2-rich (>1.5 wt%) flood basalts within the Maritimes Basin during the Early Carboniferous (La Flèche et al. 1998; Dessureau et al. 2000). It is thought that the flood basalt province was related to a mantle plume that migrated across the region (Murphy et al. 1999; Dessureau et al. 2000). It is possible that the mantle plume contributed (via mafic magma injection) to regional scale crustal melting prior to the eruption of the flood basalts and produced the silicic batholiths (Murphy et al. 1999; Shellnutt and Dostal 2015). We suggest that additional enrichment of the NENA basalts may, in part, be related to mixing with melts derived from underplated mafic rocks associated with the Maritimes Basin basalts and/or the melt-extracted Maritimes Basin mantle source. The Early Carboniferous magmatism, whether mantle plume-derived or not, was spatially restricted to the Northern Appalachians and did not affect regions south of New England (New Hampshire/Vermont) as there is no evidence of Late Devonian magmatism in Pennsylvania, New Jersey, Maryland or Virginia.

Tectonic synthesis

In this section, we present a synthesis of the Paleozoic regional tectonic and structural evolution of Eastern North America that summarizes the factors that likely contributed to the modification of the mantle sources beneath the Northern (A–A′) and Southern (B–B′) Appalachians (Fig. 11). The two profiles are depicted in a series of tectonic evolution diagrams that span from ~450 to ~200 Ma and outline the major differences in the tectonic events of each region (Fig. 12).

Structurally, the Northern Appalachians vary markedly from the southern and central Appalachians both in tectonostratigraphic component and deformation sequences (Fig. 12a, b). The difference is attributed to the shape of the original Laurentian continental margin, the shape of the Gondwana indenter, and the timing and nature of accretionary processes of the accreted terranes composed of recycled Grenville basement, Laurentian metasedimentary oceanic and arc-affinity material (Keller and Hatcher 1999). A series of episodic compressional events following the rifting of Rodinia began in the Ordovician and spanned much of the Palaeozoic era. The Taconic orogeny (Middle Ordovician—about 460 million years ago) resulted from the convergence of the Theia Sea, where earlier formed island arcs were obducted onto the Laurentian continental margin (Hatcher and Odom 1980; Faill 1997a, b, c). It consists of a complex series of orogenic events varying in intensity through time and along the orogen in eastern North America. The evidence for this orogeny is most pronounced in the northern Appalachians, but its affects stretch south to Tennessee in the Valley and Ridge province and Georgia in the Piedmont province (Glover et al. 1983; Dalziel et al. 1994; Faill 1997a). The Acadian Orogeny followed the Taconian (Early to Late Devonian—408–360 million years) and resulted from collision of the north-eastern portion of the North

Table 3 Results of trace element modeling of the ENA flood basalts

Model	Source			Partition coefficient				Bulk D			Model			
	TiO_2 (wt%)	La (ppm)	Yb (ppm)	Ol (52%)	Opx (25%)	Cpx (18%)	Sp (5%)	Gt (1%)	TiO_2	La	Yb	TiO_2 (wt%)	La (ppm)	Yb (ppm)
South	0.20	0.648	0.441	0.007	0.0003	0.056	0.01		0.189	0.014	0.133			
5%												0.88	10.19	2.50
10%												0.75	5.74	2.01
15%												0.65	4.00	1.68
25%												0.51	2.49	1.26
5%	0.20	0.648	0.441	0.007	0.0003	0.056		0.001	0.191	0.014	0.218	0.87	10.21	1.72
10%												0.74	5.75	1.49
15%												0.64	4.00	1.32
25%												0.51	2.49	1.07
Central	0.25	1.49	0.55	0.007	0.0003	0.056	0.01		0.189	0.014	0.133			
5%												1.09	23.43	3.12
10%												0.93	13.20	2.50
15%												0.81	9.19	2.09
25%												0.64	5.71	1.57
30%												0.58	4.81	1.40
North	0.35	2.33	0.65	0.007	0.0003	0.056	0.01		0.189	0.014	0.133			
5%												1.53	36.65	3.68
10%												1.30	20.64	2.96
15%												1.13	14.37	2.47
25%												0.89	8.94	1.86
30%												0.81	7.52	1.65

Modeling was calculated using $C_L = C_{mantle}/[D(1 - F) + F]$ where *CL* liquid concentration of element, C_{mantle} mantle composition of element, Bulk *D* is the bulk distribution coefficient, *F* weight fraction of melt produced. Weight fraction of *ol* olivine = 52%, *opx* orthopyroxene = 25%, *cpx* clinopyroxene = 18 wt%, *sp* spinel = 5 or 4%; *gt* garnet = 1%. The mantle composition of the Southern Appalachian models is the primitive mantle value of McDonough and Sun (1995). The mantle composition of the Northern Appalachians is from sample X-30 of Mukasa et al. (2007). The mantle composition of the Central Appalachians is the average between primitive mantle of McDonough and Sun (1995) and sample X-30 of Mukasa et al. (2007)

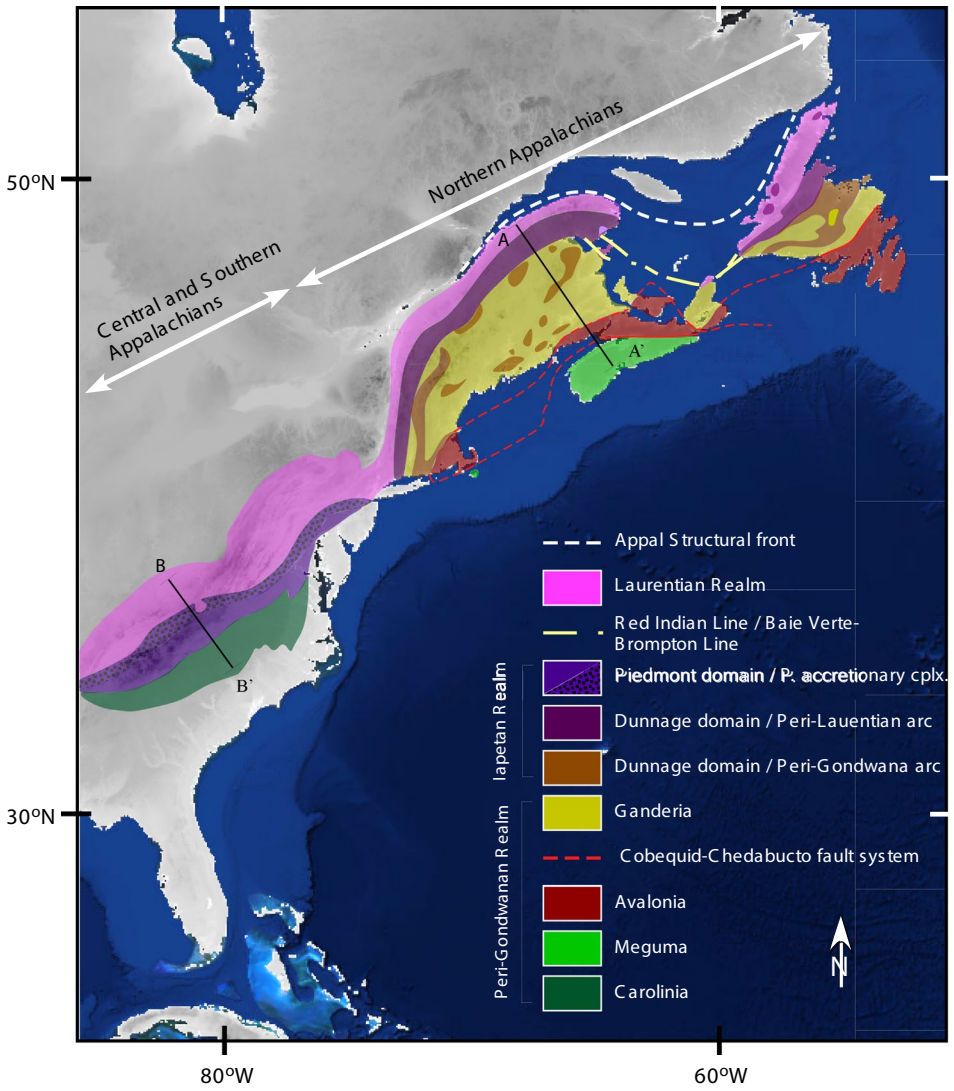

Fig. 11 Topographic map showing major lithotectonic provinces and boundary fault systems of the Appalachian orogeny. Modified from Hibbard et al. (2003, 2007) and van Staal and Barr (2012). The detailed evolution of the two profiles (A–A′ and B–B′) is shown in Fig. 12. *Appal Structural front* Appalachian Structural front, *P. accretionary cplx* post-accretionary complex

American Plate (Laurentia) with Western Europe affecting the north Appalachians from New York to Newfoundland (Rodgers 1987; Dalziel et al. 1994; Faill 1997b). The subsequent Alleghanian Orogeny (Late Carboniferous to early Triassic—300–250 million years ago) resulted from collision of the central and southern Laurentian continental margin with West Gondwana (Bradley 1989; Dalziel et al. 1994). This collision led to the formation of the Pangea supercontinent, with d'ecollement tectonism mostly in the central and southern Appalachians (Faill 1997c). Late Palaeozoic folding and igneous intrusion along the east coast of New England and parts of Atlantic Canada occurred (Bradley 1989). The age of these orogenies decreases eastward across the orogenic belt, suggesting that there was progressive eastward addition of arcs and continental fragments to the continental margin of North America (Zen 1968).

Widespread regional metamorphism and ductile deformation resulting from the Taconic orogeny were observed throughout the piedmont of the central and southern Appalachians. Radiometric age determinations (U/Pb zircon ages) indicate two major thermal events within the Baltimore Gneiss, north-eastern Maryland. The first event ranged from 1000 to 1200 Ma and occurred during the Greenville Orogeny. The second event ranged from 420 to 450 Ma (Tilton

Salinic Orogeny (442-425 Ma)

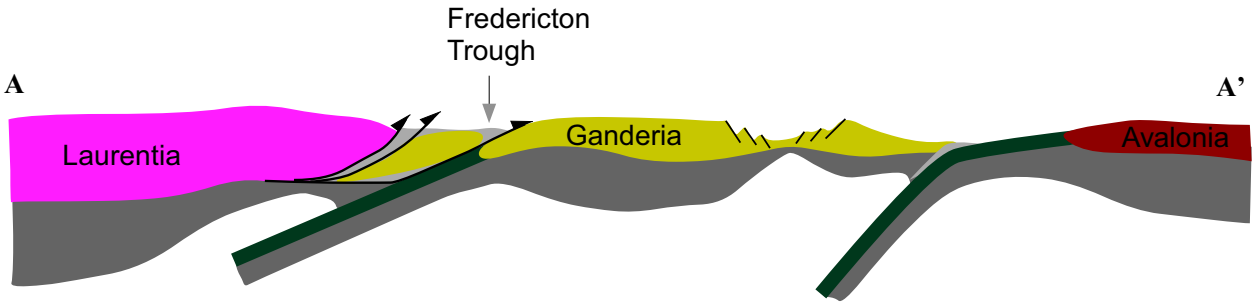

Acadian Orogeny (419-400 Ma)

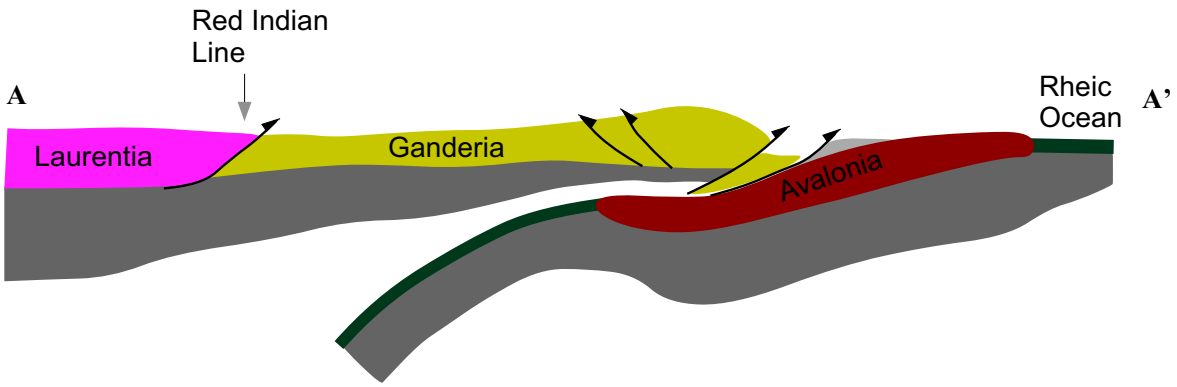

Neoacadian Orogeny (380-370 Ma)

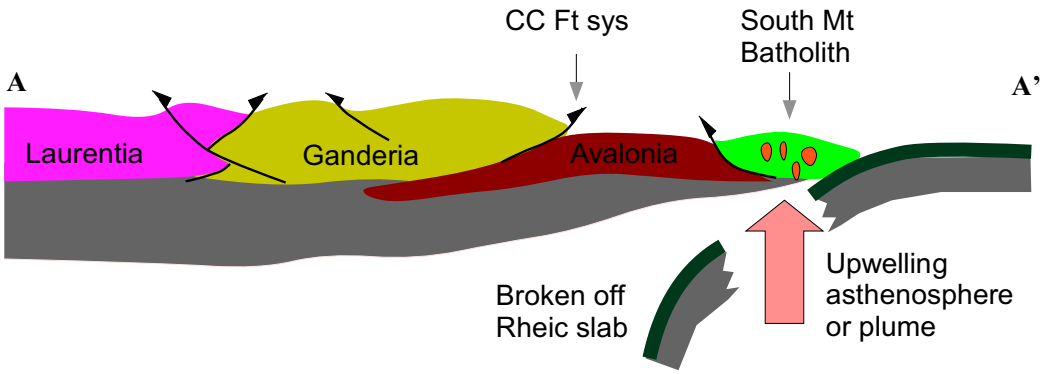

Opening of the Atlantic Ocean (225-145 Ma)

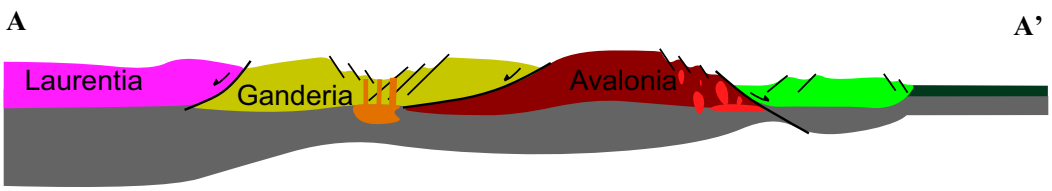

◀ **Fig. 12** **a** Sketch diagram illustrating the tectonic evolution of the Northern Appalachian orogeny along transect AA' over the Salinic (442–425 Ma), Acadian (419–400 Ma) and Neoacadian (380–370 Ma) orogeny. Modified from van Staal and Barr (2012) and Hibbard et al. (2007). **b** Sketch diagram illustrating the tectonic evolution of the Central and Southern Appalachian orogeny along transect BB′ over the Taconic (455–443 Ma), Acadian–Neoacadian (419–400 Ma), Late Missisippian–Early Pennsylvanian (325–300 Ma), and Alleghenian (300–260 Ma) orogeny. Modified from Hatcher (1978), Murphy et al. (2010), and Tremblay and Pinet (2016)

et al. 1970; Grauert 1973a, b, 1974; Muller and Chapin 1984; Stamatakos et al. 1996; Aleinikoff et al. 2002) and occurred during the Taconic Orogeny. Rb–Sr mineral ages (425–470 Ma) from a relatively undeformed pegmatite cutting the regional Glenarm schistosity after the formation of early folds (Glover et al. 1983) suggest that the peak of amphibolite facies metamorphism occurred from late Middle to early Late Ordovician time. Similar U/Pb zircon ages (489 Ma—crystallization age; 453 Ma—metamorphic age) were also recorded from the juxtaposed Baltimore mafic complex within the Glenarm series (Sinha et al. 1997). Localized retrograde metamorphism after the Ordovician thermal peak affects the Glenarm series to varying degrees (Wetherill et al. 1966, 1968; Muth et al. 1979). Young Rb/Sr biotite ages (290 Ma; Wetherill et al. 1968) reveal that the temperatures remained high enough for strontium diffusion after the Ordovician thermal peak until almost the late Pennsylvanian. This suggests that metamorphism extended from the Taconian to the Acadian Orogenies, accompanied deformation and produced widespread garnet-, staurolite-, kyanite-, and fibrolitic sillimanite bearing assemblages in the Glenarm series (Tilton et al. 1970; Grauert 1973a, b; Muller and Chapin 1984). Alleghanian cooling ages associated with later faulting are also suggested (Lang 1990; Muller and Chapin 1984). The deformation age is progressively younger to the east for the northern Appalachians yet the central and southern Appalachians progressively youngs westward (Hatcher and Odom 1980).

Post-Alleghanian–Variscan orogeny, eastern North America became a passive margin during the early Mesozoic as the Atlantic Ocean opened and Pangaea began to break-up. The extensional stress setting reactivated Paleozoic structural weak zones (e.g., Cobequid fault zone in Nova Scotia) that became the North American rift system, with rift basins and widespread mafic volcanism (Geoffroy 2005; Whithjack et al. 2012; Melankholina and Sushchevskaya 2015). Whithjack et al. (2012) separated the Jurassic CAMP-related magmatic activity along the eastern North American rift system into three regions of North, Central, and South, which correlate to our north, central, and south segments of the Appalachians. The north segments are composed of NE-SW Avalon dyke and lava flow sequences within Newfoundland and Jeanne d'Arc basin. Less intense magmatism is noted for the central and southern segment, but are composed of wide spread N to NE striking dyke, thick lava flow sequences, and intrusive sheets. However, no lava flow sequences are noted for the southern segment.

Melankholina and Sushchevskaya (2015) pointed out that there is a dissimilar isotopic composition among the north verses central segments magmatism. We consider the compositional differences between the Southern and Northern Appalachian basalts are probably related to the specific tectonomagmatic evolution of the accreted terranes (Carolinia and West Avalonia) as they each rifted from Gondwana and accreted to Laurentia during the Neoproterozoic to Late Palaeozoic (Murphy and Nance 2002; Nance et al. 2002; Whalen et al. 2015). Moreover, Late Devonian–Early Carboniferous magmatism in New England and Atlantic Canada was an additional influence of Middle Mesozoic mantle melting in the north (Fig. 12a). As tensional plate stresses acted on Pangaea during the Early Jurassic, rifting and basin formation was initiated followed by mantle melting and the eruption of the ENA basalts and emplacement of mafic dykes (Dostal and Durning 1998; Pe-Piper and Reynolds 2000). It is likely that the Southern basalts were derived by partial melting of a mantle source beneath Carolinia that was less affected by subduction and accretion, whereas the Northern basalts were derived by partial melting of mantle beneath West Avalonia that experienced melting associated with subduction and upwelling mantle and rifting during the Late Devonain to Early Carboniferous (Murphy et al. 2011; Callegaro et al. 2013; Merle et al. 2013; Whalen et al. 2015).

Conclusions

Basaltic rocks from the Early Jurassic ENA sub-province of the CAMP were likely produced under a thermal regime that was between ambient mantle conditions ($T_P \approx 1440$ °C) and hot mantle. The thermal conditions are consistent with melting above a passive extensional tectonic setting rather than an active mantle plume setting. The rocks from the Northern Appalachians were likely derived from an Fe-rich (FeOt = 8.6 wt%) 'mantle wedge-type' source that was affected by a Late Devonian–Early Carboniferous mantle plume. In contrast, the rocks from the Southern Appalachians were derived primarily from spinel peridotite that had less FeOt (FeOt = 8.3 wt%) and was not affected by Late Devonian-Early Carboniferous magmatism. The spatial-compositional variation of the ENA basaltic rocks is attributed to differing amounts of melting from mantle sources

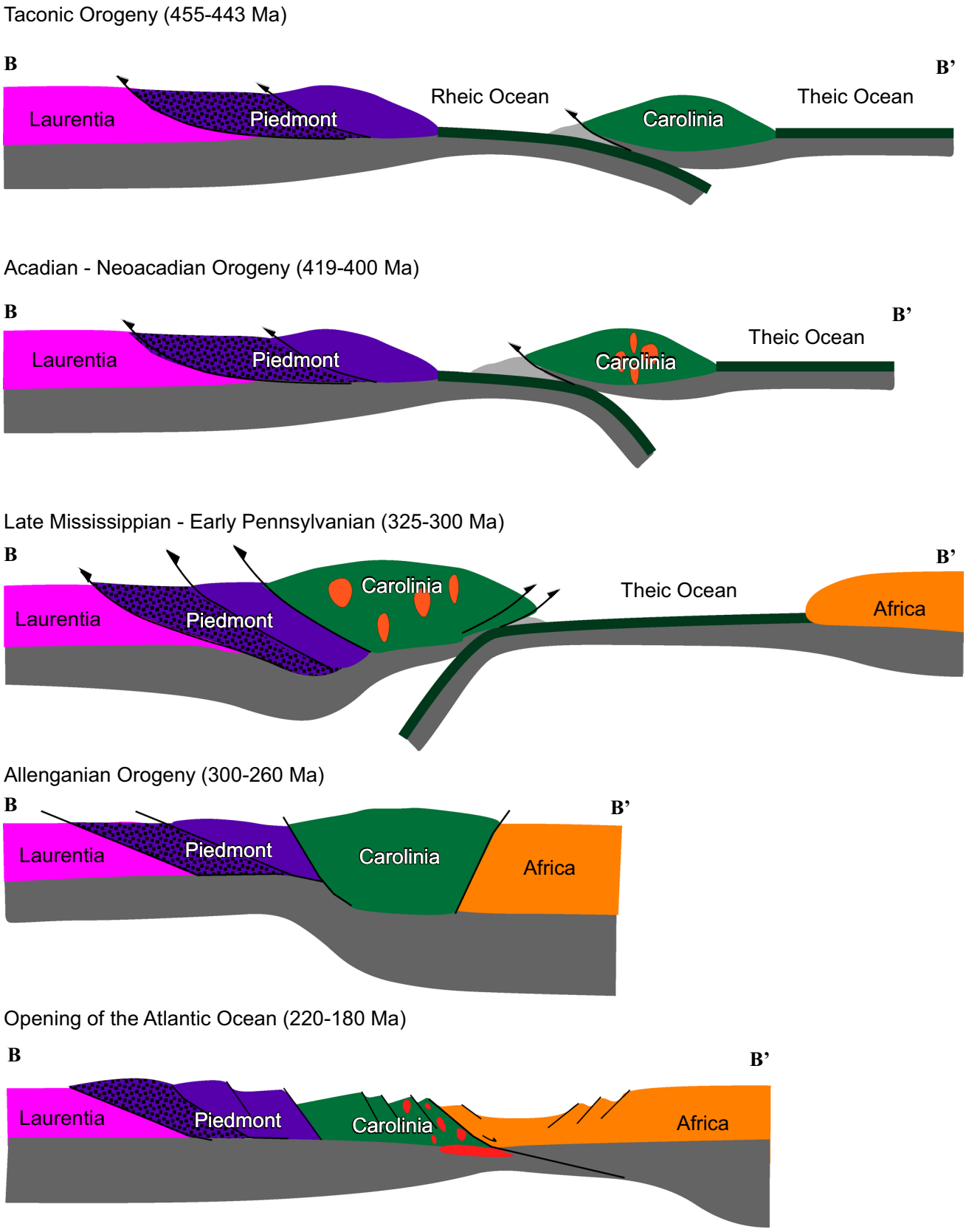

Fig. 12 (continued)

that experienced regionally unique subduction-related mantle enrichment prior to and during the accretion of Gondwanan terranes (Carolinia and West Avalonia) to eastern North America.

Acknowledgements We thank Marcos Zentilli and Ali Polat for their constructive reviews and John Greenough (Guest Editor) and Christian Dullo (Chief Editor) for editorial handling. Dan Kontak provided additional field photographs of the NMB. JGS would like to acknowledge the support of the Ministry of Science and Technology of Taiwan through Grant 102-2628-M-003-001-MY4. JD acknowledges the support of the National Sciences and Engineering Research Council (Canada) Discovery grant.

References

Aleinikoff JN, Wintsch RP, Fanning CM, Dorais MJ (2002) U-Pb geochronology of zircon and polygenetic titanite from the Glastonbury Complex, Connecticut, USA: an integrated SEM, EMPA, TIMS, and SHRIMP study. Chem Geol 188:125–147

Aumento F (1966) Zeolite minerals, Nova Scotia. In: Geology of parts of the Atlantic Provinces. Geol Assoc Canada-Mineral Assoc Canada Field Trip, vol 3. pp 71–94

Arth JG (1976) Behaviour of trace elements during magmatic processes—a summary of theoretical models and their applications. J Res USGS 4:41–47

Ayer JA, Davis DW (1997) Neoarchean evolution of differing convergent margin assemblages in the Wabigoon Subprovince: geochemical and geochronological evidence from the Lake of the Woods greenstone belt, Superior Province, northwestern Ontario. Precambrian Res 8:155–178

Beattie P (1994) Systematics and energetics of trace-element partitioning between olivine and silicate melts: implications for the nature of mineral/melt partitioning. Chem Geol 117:57–71

Blackburn TJ, Olsen PE, Bowring SA, McLean NM, Kent DV, Puffer J, McHone G, Rasbury ET, Et-Touhami M (2013) Zircon U-Pb geochronology links the end-Triassic extinction with the Central Atlantic Magmatic Province. Science 340:941–945

Bowen NL (1916) Discussion of "Magmatic differentiation in effusive rocks". Trans Am Inst Mining Eng 54:455–457

Bradley DC (1989) Taconic plate kinematics as revealed by foredeep stratigraphy, Appalachian orogen. Tectonics 8(5):1037–1049

Callegaro S, Marzoli A, Bertrand H, Chiaradia M, Reisberg L, Meyzen C, Bellieni G, Weems RE, Merle R (2013) Upper and lower crust recycling in the source of CAMP basaltic dykes from southeastern North America. Earth Planet Sci Lett 376:186–199

Callegaro S, Rapaille C, Marzoli A, Bertran H, Chiaradia M, Reisberg L, Bellieni G, Martins L, Madeira J, Mata J, Youbi N, De Min A, Azeveda MR, Bensalah MK (2014) Enriched mantle source for the Central Atlantic magmatic province: new supporting evidence from southwestern Europe. Lithos 188:15–32

Cebriá JM, López-Ruiz J, Doblas M, Martins LT, Munha J (2003) Geochemistry of the Early Jurassic Messejana–Plasencia dyke (Portugal–Spain); implications on the origin of the Central Atlantic Magmatic Province. J Petrol 44:547–568

Chowns TM, Williams CT (1983) Pre-Cretaceous rocks beneath the Georgia Coastal Plain—Regional implications. In: Gohn GS (ed) Studies related to the Charleston, South Carolina earthquake of 1886—tectonics and seismicity, US Geol Surv Prof Pap, vol 1313-L. United States Geological Survey, Washington, DC, pp L1–L39

Cirilli S, Marzoli A, Tanner L, Bertrand H, Buratti N, Jourdan F, Bellieni G, Kontak D, Renne PR (2009) Latest Triassic onset of the Central Atlantic Magmatic Province (CAMP) volcanism in the Fundy Basin (Nova Scotia): new stratigraphic constraints. Earth Planet Sci Lett 286:514–525

Coltice N, Phillips BR, Bertrand H, Richard Y, Rey P (2007) Global warming of the mantle at the origin of flood basalts over supercontinents. Geology 35:391–394

Cummins LE, Arthur JD, Ragland PC (1992) Classification and tectonic implications for early Mesozoic magma types of the circum-Atlantic. In: Puffer JH, Ragland PC (eds) Eastern North America Mesozoic Magmatism. Geol Soc Am Spec Pap, vol 268. Geological Society of America, Boulder, Colorado, pp 119–135

Dalziel IWD, Dalla LH, Gahagan LM (1994) Paleozoic Laurentia–Gondwana interaction and the origin of the Appalachian—Andean mountain system. Geol Soc Am Bull 106:243–252

Dawson JB (2002) Metasomatism and partial melting in upper-mantle peridotite xenolihs from Lashaine Volcano, northern Tanzania. J Petrol 43:1749–1777

Dennis AJ, Shervais JW (1996) The Carolina terrane in northwestern South Carolina: insights into the development of an evolving island arc. In: Nance RD, Thompson MD (eds) Avalonian and related Peri-Gondwana Terranes of the Circum–North Atlantic. Geol Soc Am Spec Pap, vol 304. Geological Society of America, Boulder, Colorado, pp 237–256

Dennis AJ, Wright JE (1997) The Carolina terrane in northwestern South Carolina, U.S.A.: late Precambrian–Cambrian deformation and metamorphism in a peri-Gondwana oceanic arc. Tectonics 16:460–473

Dessureau G, Piper DJW, Pe-Piper G (2000) Geochemical evolution of earliest Carboniferous continental tholeiitic basalts along a crustal-scale shear zone, southwestern Maritimes basin, eastern Canada. Lithos 50:27–50

Dorais MJ (2003) The petrogenesis and emplacement of the New Hampshire plutonic suite. Am J Sci 303:447–487

Dorais MJ, Paige ML (2000) Regional geochemical and isotopic variations of northern New England plutons: implications for magma sources and for Grenville and Avalon basement-terrane boundaries. Geol Soc Am Bull 112:900–914

Dostal J, Dupuy C (1984) Geochemistry of the North Mountain basalts, Nova Scotia, Canada. Chem Geol 45:245–261

Dostal J, Durning M (1998) Geochemical constraints on the origin and evolution of early Mesozoic dikes in Atlantic Canada. Eur J Mineral 10:79–94

Dostal J, Greenough JD (1992) Geochemistry and petrogenesis of the early Mesozoic North Mountain basalts of Nova Scotia, Canada. In: Puffer JH, Ragland PC (eds) Eastern North America Mesozoic Magmatism. Geol Soc Am Spec Pap, vol 268. Geological Society of America, Boulder, Colorado, pp 149–159

Dostal J, Dupuy C, Caby R (1994) Geochemistry of the Neoproterozoic Tilemsi belt of Iforas (Mali, Sahara): a crustal section of an oceanic island arc. Precambrian Res 65:55–69

Dostal J, Keppie JD, Wilson RA (2016) Nd isotopic and trace element constraints on the source of Silurian-Devonian mafic lavas in the Chaleur Bay Synclinorium of New Brunswick (Canada): tectonic implications. Tectonophysics 681:364–375

Faill RT (1997a) A geologic history of the north-central Appalachians, part 1. Orogenesis from the Mesoproterozoic through the Taconic orogeny. Am J Sci 297:551–619

Faill RT (1997b) A geologic history of the north-central Appalachians, part 2. The Appalachian basin from the Silurian through the Carboniferous. Am J Sci 297:729–761

Faill RT (1997c) A geologic history of the north-central Appalachians, Part 3. The Alleghany Orogeny. Am J Sci 297:131–179

Fan WM, Zhang CH, Wang YJ, Guo F, Peng TP (2008) Geochronology and geochemistry of Permian basalts in western Guangxi Province, Southwest China: evidence for plume–lithosphere interaction. Lithos 102:218–236

Froelich AJ, Olsen PE (1985) Newark Supergroup, a revision of the Newark Group in eastern North America. In: Robinson GR, Froelich AJ (eds) Proceedings, 2nd United States Geological Survey workshop on the early Mesozoic basins of the eastern United States. US Geol Sur Circular, vol 946. United States Geological Survey, Reston, Virginia, pp 36–45

Fujimaki H, Tatsumoto M, Ki Aoki (1984) Partition coefficients of Hf, Zr, and REE between phenocrysts and groundmasses. J Geophys Res 89:662–672

Geoffroy L (2005) Volcanic passive margins. C R Geosci 337:1395–1408

Glover L, Speer AG, Russell S, Farrar S (1983) Ages of regional metamorphism and ductile deformation in the central and southern Appalachians. Lithos 16:223–243

Grauert B (1973a) U-Pb isotopic studies of zircons from the Baltimore gneiss of the Townson Dome, Maryland. Year B Carnegie Inst Wash 72:285–288

Grauert B (1973b) U-Pb isotopic studies of zircons from the Gunpowder granite, Baltimore County, Maryland. Year B Carnegie Inst Wash 72:288–293

Grauert B (1974) U-Pb systematics in heterogeneous zircon populations from the Precambrian basement of the Maryland Piedmont. Earth Planet Sci Lett 23:238–248

Green TH, Sie SH, Ryan CG, Cousens DR (1989) Proton microprobe-determined partitioning of Nb, Ta, Zr, Sr and Y between garnet, clinopyroxene and basaltic magma at high pressure and temperature. Chem Geol 74:201–216

Green T, Blundy J, Adam J, Yaxley G (2000) SIMS detemination of trace element partition coefficients between garnet, clinopyroxene and hydrous basaltic liquids at 2–7.5 GPa and 1080–1200 °C. Lithos 53:165–187

Greenough JD, Dostal J (1992a) Layered rhyolite bands in a thick North Mountain basalt flow: the products of silicate liquid immiscibility. Mineral Mag 56:309–318

Greenough JD, Dostal J (1992b) Cooling history and differentiation of a thick North Mountain basalt flow (Nova Scotia, Canada). Bull Volcanol 55:63–73

Greenough JD, Hodych JP (1990) Evidence for lateral magma injection in the Early Mesozoic dykes of Eastern North America. In: Parker AJ, Rickwood PC, Tucker DH (eds) Mafic dykes and emplacement mechanisms. Proc Second Internat Dyke Conf Balkema, Rotterdam, pp 35–46

Grossman JN, Gottfried D, Froelich AJ (1991) Geochemical data for the Jurassic diabase associated with Early Mesozoic basins in the eastern United States. US Geol Sur Op File Rep 91-322-J, United States Geological Survey, Reston, Virginia

Hatcher RDJ (1978) Tectonics of the western Piedmont and Blue Ridge: review and speculation. Am J Sci 278:276–304

Hatcher RD, Odom AL (1980) Timing of thrusting in the southern Appalachians, USA: model for orogeny? J Geol Soc Lond 137:321–327

He Q, Xiao L, Balta B, Gao R, Chen J (2010) Variety and complexity of the Late-Permian Emeishan basalts: reappraisal of plume–lithosphere interaction processes. Lithos 119:91–107

Heatherington AL, Mueller PA (1999) Lithospheric source of North Florida, USA tholeiites and implications for the origin of the Suwannee terrane. Lithos 46:215–233

Heatherington AL, Mueller PA (2003) Mesozoic igneous activity in the Suwannee Terrane, southeastern USA: petrogenesis and Gondwanan affinities. Gondwana Res 6:296–311

Herzberg C, Asimow PD (2008) Petrology of some oceanic island basalts: PRIMELT2.XLS software for primary magma calculation. Geochem Geophys Geosyst 9:Q09001. doi:10.1029/2008GC002057

Herzberg C, Asimow PD (2015) PRIMELT3 MEGA.XLSM software for primary magma calculation: peridotite primary magma MgO contents from the liquids to the solidus. Geochem Geophys Geosyst 16:563–578

Herzberg C, Gazel E (2009) Petrological evidence for secular cooling in mantle plumes. Nature 458:619–622

Herzberg C, O'Hara MJ (2002) Plume-associated ultramafic magmas of Phanerozoic age. J Petrol 43:1857–1883

Herzberg C, Asimow PD, Arndt N, Niu Y, Lesher CM, Fitton JG, Cheadle MJ, Saunders AD (2007) Temperatures in ambient mantle and plumes: constraints from basalts, picrites, and komatiites. Geochem Geophys Geosyst 8:Q02006. doi:10.1029/2006GC001390

Hibbard J, Standard I, Miller B, Hames W, Lavallee S (2003) Regional significance of the Gold Hill fault zone, Carolina zone of North Carolina. Geol Soc Am Abs Prog vol 35. Geological Society of America, Boulder, Colorado, p 24

Hibbard JP, van Staal CR, Miller BV (2007) Links among Carolinia, Avalonia, and Ganderia in the Appalachian peri-Gondwanan realm. In: Sears JW, Harms TA, Evenchick CA (eds) Whence the Mountains? Inquiries into the evolution of orogenic systems: a volume in honor of Raymond A. Price. Geol Soc Am Spec Pap, vol 433, pp 291–311

Hodych JP, Dunning GR (1992) Did the Manicouagan impact trigger end-of-Triassic mass extinction? Geology 20:51–54

Hole MJ (2015) The generation of continental flood basalts by decompressional melting of internally heated mantle. Geology 43:311–314

Ionov DA, Bodinier JL, Mukasa SB, Zanetti A (2002) Mechanism and source of mantle metasomatism: major and trace element compositions of peridotite xenoliths from Spitsbergen in the context of numerical modeling. J Petrol 43:2219–2259

Irving AJ, Frey FA (1978) Distribution of trace elements between garnet megacrysts and host volcanic liquids of kimberlitic to rhyolitic composition. Geochim Cosmochim Acta 42:771–787

Janney PE, Castillo PR (2001) Geochemistry of the oldest Atlanitc oceanic crust suggest mantle plume involvement in the early history of the central Atlantic Ocean. Earth Planet Sci Lett 192:291–302

Jenner GA, Foley SF, Jackson SE, Green TH, Fryer BJ, Longerich HP (1994) Determination of partition coefficients for trace elements in high pressure-temperature experimental run products by laser ablation microprobe-inductively coupled plasma-mass spectrometry (LAM-ICP-MS). Geochim Cosmochim Ac 57:5099–5103

Jochum KP, Arndt NT, Hofmann AW (1991) Nb–Th–La in komatiites and basalts: constraints on komatiite petrogenesis and mantle evolution. Earth Planet Sci Lett 107:272–291

Johnson KTM (1994) Experimental cpx/and garnet/melt partitioning of REE and other trace elements at high pressures: petrogenetic implications. Mineral Mag 58:454–455

Keller GR, Hatcher RD Jr (1999) Some comparisons of the structure and evolution of the southern Appalachian–Ouachita orogen and portions of the Trans-European Suture Zone region. Tectonophysics 314:43–68

Klemme S, Gunther D, Hametner K, Prowatke S, Zack T (2006) The partitioning of trace elements between ilmenite, ulvospinel, armalcolite and silicate melts with implications for the early differentiation of the moon. Chem Geol 234:251–263

Kononova VA, Kurat G, Embey-Isztin A, Pervov VA, Koeberl C, Brandstätter F (2002) Geochemistry of metasomatised spinel peridotite xenoliths from the Dariganga Plateau, South-eastern Mongolia. Mineral Petrol 75:1–21

Kontak DJ, Archibald DA (2003) $^{40}Ar/^{39}Ar$ age dating of the Jurassic North Mountain Basalt, southern Nova Scotia. Atl Geol 39:47–54

Kontak DJ, Dostal J, Greenough J (2005) Geology and volcanology of the Jurassic North Mountain Basalt, southern Nova Scotia. In: Geological Association of Canada-Mineralogical Association of Canada annual meeting, Field Trip B3. At Geosci Soc Spec Pub 29, Atlantic Geoscience Society, Halifax, Nova Scotia

La Flèche MR, Camiré G, Jenner GA (1998) Geochemistry of post-Acadian, Carboniferous continental intraplate basalts from the Maritimes Basin, Magdalen Islands, Québec, Canada. Chem Geol 148:115–136

Lang HM (1990) Regional variation in metamorphic conditions recorded by pelitic schists in the Baltimore Area, Maryland. Southeast Geol 31:27–43

Le Bas MJ (2000) IUGS reclassification of the high-Mg and picritic volcanic rocks. J Petrol 41:1467–1470

Mallmann G, O'Neill HStC (2009) Mantle melting as a function of oxygen fugacity compared with some other elements (Al, P, Ca, Sc, Ti, Cr, Fe, Ga, Y, Zr and Nb). J Petrol 50:1765–1794

Marzoli A, Renne PR, Piccirillo EM, Ernesto M, Bellieni G, De Min A (1999) Extensive 200-million-year-old continental flood basalts of the Central Atlantic Magmatic Province. Science 284:616–618

Marzoli A, Bertrand H, Knight KB, Cirilli S, Buratti N, Verati C, Nomade S, Renne PR, Youbi N, Martini R, Allenbach K, Neuwerth R, Rapaille C, Zaninetti L, Bellieni G (2004) Synchrony of the Central Atlantic magmatic province and the Triassic–Jurassic boundary climatic and biotic crisis. Geology 32:973–976

Marzoli A, Jourdan F, Puffer JH, Cuppone T, Tanner LH, Weems RE, Bertran H, Cirilli S, Bellieni G, De Min A (2011) Timing and duration of the Central Atlantic magmatic province in the Newerk and Culpeper basins, eastern USA. Lithos 122:175–188

McDonough WF (1990) Constraints on the composition of the continental lithospheric mantle. Earth Planet Sci Lett 101:1–18

McDonough WF, Sun SS (1995) The composition the Earth. Chem Geol 120:223–253

McHone JG (2000) Non-plume magmatism and rifting during the opening of the central Atlantic Ocean. Tectonophysics 316:287–296

McKenzie D, O'Nions RK (1991) Partial melt distributions from inversion of rare earth element concentrations. J Petrol 32:1021–1091

Melankholina EN, Sushchevskaya NM (2015) Development of passive margins of the Central Atlantic and initial opening of ocean. Geotectonics 49:75–92

Menzies MA, Leeman WP, Hawkesworth CJ (1983) Isotope geochemistry of Cenozoic volcanic rocks reveals mantle heterogeneity below western USA. Nature 303:205–209

Merle R, Marzoli A, Reisberg L, Bertrand H, Nemchin A, Chiaradia M, Callegaro S, Jourdan F, Bellieni G, Kontak D, Puffer J, McHone JG (2013) Sr, Nd, Pb and Os isotopic systematics of CAMP tholeiites from eastern North America (ENA): evidence of a subduction-enriched mantle source. J Petrol 55:133–180

Mukasa SB, Blatter DL, Andronikov AV (2007) Mantle peridotite xenoliths in andesite lava at El Peñon, central Mexican volcanic belt: isotopic and trace element evidence for melting and metasomatism in the mantle wedge beneath and active arc. Earth Planet Sci Lett 260:37–55

Muller PD, Chapin DA (1984) Tectonic evolution of the Baltimore gneiss anticlines, Maryland. Geol Soc Am Spec Pap 194:127–148

Murphy JB, Nance RD (2002) Sm–Nd isotopic systematics as tectonic tracers: an example from West Avalonia in the Canadian Appalachians. Earth Sci Rev 59:77–100

Murphy JB, van Staal CR, Keppie JD (1999) Middle to late Paleozoic Acadian orogeny in the northern Appalachians: a Laramide-style plume-modified orogeny? Geology 27:653–656

Murphy JB, Keppie JD, Nance RD, Dostal J, Creaser RA (2010) Comparative evolution of the Iapetus and Rheic Oceans: a North America perspective. Gondwana Res 17:482–499

Murphy JB, Dostal J, Gutiérrez-Alonso G, Keppie JD (2011) Early Jurassic magmatism on the northern margin of CAMP: derivation from a Proterozoic sub-continental lithospheric mantle. Lithos 123:158–164

Muth K, Arth JG, Reed JCJ (1979) A minimum age for high-grade metamorphism and granite intrusion in the Piedmont of the Potomac River Gorge near Washington, DC. Geology 7:349–350

Nance RD, Murphy JB, Keppie JD (2002) A Cordilleran model for the evolution of Avalonia. Tectonophysics 352:11–31

O'Reilly SY, Griffin WL (2013) Mantle Metasomatism. In: Harlov DE, Austrheim H (eds) Metasomatism and the chemical transformation of rock. Lecture notes in earth system sciences, Springer, Verlag, Berlin, Heidelberg, pp 471–533

Olsen PE (1997) Stratigraphic record of the early Mesozoic breakup of Pangea in the Laurasia-Gondwana rift system. Annu Rev Earth Planet Sci 25:337–401

Olsen PE, McCune AR, Thomson KS (1982) Correlation of the early Mesozoic Newark Supergroup by vertebrates, principally fishes. Am J Sci 282:49–86

Olsen PE, Shubin NH, Anders MH (1987) New early Jurassic tetrapod assemblages constrain Triassic-Jurassic tetrapod extinction event. Science 237:1025–1029

Olsen PE, Schlische RW, Fedosh MS (1998) 580 ky duration of the Early Jurassic flood basalt event in eastern North America estimated using Milankovitch cyclostratigraphy. In: Morales M (ed) The Continental Jurassic. Mus Nor Arizona Bull, vol 60. Northern Arizona Society of Science and Art, Flagstaff, Arizona, pp 11–22

Pegram WJ (1990) Development of continental lithospheric mantle as reflected in the chemistry of the Mesozoic Appalachian tholeiites, U.S.A. Earth Planet Sci Lett 97:316–331

Pe-Piper G, Reynolds PH (2000) Early Mesozoic alkaline mafic dykes, southwestern Nova Scotia, Canada, and their bearing on Triassic–Jurassic magmatism. Can Mineral 38:217–232

Pe-Piper G, Jansa LF, Lambert RSJ (1992) Early Mesozoic magmatism on theeastern Canadian margin: petrogenetic and tectonic significance. In: Puffer JH, Ragland PC(eds) Eastern North America Mesozoic Magmatism, vol 268. Geological Society of America Special Papers, Boulder, Colorado, pp 13–36

Powers S (1916) The Acadian Triassic. J Geol 24:1–26

Powers S, Lane AC (1916) Magmatic differentiation in effusive rocks. Trans Am Inst Mining Eng 54:442–455

Puffer JH (1992) Eastern North America flood basalts in the context of the incipient breakup of Pangea. In: Puffer JH, Ragland PC (eds) Eastern North America Mesozoic Magmatism. Geol Soc Am Spec Pap, vol 268. Geological Society of America, Boulder, Colorado, pp 95–118

Puffer JH (2001) Contrasting high field strength element contents of continental flood basalts from plume versus reactivated-arc sources. Geology 29:675–678

Rodgers J (1987) The Appalachian–Ouachita orogenic belt. Episodes 10:259–266

Salters V, Longhi J (1999) Trace element partitioning during the initial stages of melting beneath mid-ocean ridges. Earth Planet Sci Lett 166:15–30

Schlische RW, Withjack MO, Eisenstadt G (2002) An experimental study of the secondary deformation produced by oblique-slip normal faulting. Am Assoc Pet Geol Bull 86:885–906

Shellnutt JG, Dostal J (2015) Granodiorites of the South Mountain Batholith (Nova Scotia, Canada) derived by partial melting of Avalonia granulite rocks beneath the Meguma terrane: implications for the heat source of the Late Devonian granites of the North Appalachians. Tectonophysics 655:206–212

Shellnutt JG, Dostal J, Iizuka Y (2013) Evidence of silicate immiscibility within flood basalts from the Central Atlantic Magmatic Province. Geochem Geophys Geosyst 14:4921–4935

Sinha AK, Hanan B, Wayne DM (1997) Igneous and metamorphic U–Pb zircon ages from the Baltimore mafic complex, Maryland Piedmont. Geol Soc Am Mem 191:275–286

Stamatakos J, Hirt AM, Lowrie W (1996) The age and timing of folding in the central Appalachians from paleomagnetic results. Geol Soc Am Bull 108:815–829

Storey BR, Leat PL, Ferris JK (2001) The location of mantle plume centers during the initial stages of Gondwana breakup. In: Ernst RE, Buchan KL (eds) Mantle plumes: their identification through time. Geol Soc Am Spec Pap, vol 352. Geological Society of America, Boulder, Colorado, pp 71–80

Sun SS, McDonough WF (1989) Chemical and isotopic systematics of oceanic basalts: implications for mantle composition and processes. In: Saunders AD, Norry MJ (eds) Magmatism in the ocean basins. Geol Soc Lond Spec Publ, vol 42. Blackwell Scientific Publications, Oxford, UK, pp 313–345

Tilton GR, Doe BR, Hopson CA (1970) Zircon age measurements in the Maryland Piedmont with special reference to Baltimore Gneiss problems. Wiley, New York

Tomascak PB, Brown M, Solar GS, Becker HJ, Centorbu TL, Tian J (2005) Source contributions to Devonian granite magmatism near the Laurentian border, New Hampshire and western Maine, USA. Lithos 80:75–99

Tremblay A, Pinet N (2016) Late Neoproterozoic to Permian tectonic evolution of the Quebec Appalachians, Canada. Earth Sci Rev 160:131–170

van Staal CR, Barr SM (2012) Lithospheric architecture and tectonic evolution of the Canadian Appalachians and associated Atlantic margin. In: Percival JA, Cook FA, Clowes RM (eds) Tectonic styles in Canada: the LITHOPROBE perspective. Geol Assoc Can Spec Pap, vol 49. Geological Association of Canada, St. John′s, Newfoundland and Labrador, pp 41–95

Walker TL, Parsons AL (1922) The zeolites of Nova Scotia. Univ Toronto Stud Ser 14:13–73

Weigand P, Ragland PC (1970) Geochemistry of Mesozoic dolerite dikes from eastern North America. Contrib Mineral Petrol 29:195–214

Wetherill GW, Tilton GR, Davis GL, Hart SR, Hopson CA (1966) Age measurements in the Maryland Piedmont. J Geophys Res 71:2130–2155

Wetherill GW, Davis GL, Lee-Hu C (1968) Rb-Sr measurements on whole rocks and separated minerals from the Baltimore Gneiss, Maryland. Geol Soc Am Bull 79:757–762

Whalen L, Gazel E, Vidito C, Puffer J, Bizimis M, Henika W, Caddick MJ (2015) Supercontinental inheritance and its influence on supercontinental breakup: the Central Atlantic Magmatic Province and the breakup of Pangea. Geochem Geophys Geosyst 16:3532–3554

White CE, Kontak DJ, Demont GJ, Archibald D (2017) Remnants of Early Mesozoic basalt of the Central Atlantic magmatic province in Cape Breton Island, Nova Scotia, Canada. Can J Earth Sci 54:345–358

Whiteside JH, Olsen PE, Eglington T, Brookfield ME, Sambrotto RN (2010) Compound-specific carbon isotopes from Earth's largest flood basalt eruptions directly linked to the end-Triassic mass extinction. Proc Natl Acad Sci 107:6721–6725

Whithjack MO, Schlishe RW, Olsen PE (2012) Development of the passive margin of eastern North America: Mesozoic rifting, igneous activity, and breakup. In: Roberts DG, Bally AW (eds) Regional geology and tectonics: phanerozoic rift systems and sedimentary basins. Elsevier, New York, pp 305–335

Wilson M (1989) Igneous petrogenesis. Unwin Hyman, London

Wilson M (1997) Thermal evolution of the Central Atlantic passive margins: continental break-up above a Mesozoic super-plume. J Geol Soc Lond 154:491–495

Zen E (1968) Studies of Appalachian geology: northern and maritime. Wiley, New York